

Λ_s CDM cosmology: Alleviating major cosmological tensions by predicting standard neutrino properties

Anita Yadav,^{1,*} Suresh Kumar,^{2,†} Cihad Kıbrıs,^{3,‡} and Özgür Akarsu^{3,§}

¹*Department of Mathematics, Indira Gandhi University, Meerpur, Haryana 122502, India*

²*Data Science Institute, Plaksha University, Mohali, Punjab-140306, India*

³*Department of Physics, Istanbul Technical University, Maslak 34469 Istanbul, Türkiye*

In this work, we investigate a two-parameter extension of the Λ_s CDM model, as well as the Λ CDM model for comparison, by allowing variations in the effective number of neutrino species (N_{eff}) and their total mass ($\sum m_\nu$). Our motivation is twofold: (i) to examine whether the Λ_s CDM framework retains its success in fitting the data and addressing major cosmological tensions, without suggesting a need for a deviation from the standard model of particle physics, and (ii) to determine whether the data indicate new physics that could potentially address cosmological tensions, either in the post-recombination universe through the late-time ($z \sim 2$) mirror AdS-to-dS transition feature of the Λ_s CDM model, or in the pre-recombination universe through modifications in the standard values of N_{eff} and $\sum m_\nu$, or both. Within the extended Λ_s CDM model, referred to as Λ_s CDM+ N_{eff} + $\sum m_\nu$, we find no significant tension when considering the Planck-alone analysis. We observe that incorporating BAO data limits the further success of the Λ_s CDM extension. However, the weakly model-dependent BAOtr data, along with Planck and Planck+PP&SH0ES, favors an H_0 value of approximately $73 \text{ km s}^{-1} \text{ Mpc}^{-1}$, which aligns perfectly with local measurements. In cases where BAOtr is part of the combined dataset, the mirror AdS-dS transition is very effective in providing enhanced H_0 values, and thus the model requires no significant deviation from the standard value of $N_{\text{eff}} = 3.044$, remaining consistent with the standard model of particle physics. Both the H_0 and S_8 tensions are effectively addressed, with some compromise in the case of the Planck+BAO dataset. Finally, the upper bounds obtained on total neutrino mass, $\sum m_\nu \lesssim 0.50 \text{ eV}$, are fully compatible with neutrino oscillation experiments. Our findings provide evidence that late-time physics beyond Λ CDM, such as Λ_s CDM, without altering the standard description of the pre-recombination universe, can suffice to alleviate the major cosmological tensions, as indicated by our analysis of Λ_s CDM+ N_{eff} + $\sum m_\nu$.

I. INTRODUCTION

Insofar as the most contemporary observations are concerned, the energy budget of the present-day universe consists mostly of cold dark matter (CDM) and dark energy (DE). The standard Lambda Cold Dark Matter (Λ CDM) model, resting on these elusive dark constituents, has, without a doubt, provided a marvelous description of the observed cosmic phenomena, including the late-time accelerated expansion [1, 2] via its positive cosmological constant Λ assumption, cosmic microwave background (CMB) radiation [3], and its minute fluctuations, as well as the formation and growth of large-scale structures (LSS) [4–9]. As successful as it may seem, Λ CDM, has been found to be fraught with a number of cracks over the past few years. As the observational data keep growing and improving in precision, not only are brand-new discrepancies with independent observations emerging within the framework of the Λ CDM model, but some of the existing ones also escalate to higher degrees of significance [10–21]. The most notorious of them all is in the value of the Hubble constant H_0 , known as the H_0 tension [22–24]. It captures a more-than- 5σ discordance between the local

measurements by the SH0ES team using the Cepheid-calibrated distance ladder approach, which finds $H_0 = 73.04 \pm 1.04 \text{ km s}^{-1} \text{ Mpc}^{-1}$ ($73.30 \pm 1.04 \text{ km s}^{-1} \text{ Mpc}^{-1}$, when including high-redshift SN Ia) [25], and the latest measurement of $73.17 \pm 0.86 \text{ km s}^{-1} \text{ Mpc}^{-1}$ [26] (see also 73.22 ± 0.68 (stat) ± 1.28 (sys) $\text{km s}^{-1} \text{ Mpc}^{-1}$ using Cepheids, TRGB, and SBF Distance Calibration to SN Ia [27]), and the value $H_0 = 67.36 \pm 0.54 \text{ km s}^{-1} \text{ Mpc}^{-1}$ estimated by the CMB measurements assuming Λ CDM [3]. In addition to the H_0 tension, it was suggested that Λ CDM suffers from another tension, though less significant, known as the S_8 tension [16, 18–21, 28–30]. Planck- Λ CDM predicts a larger weighted amplitude of matter fluctuations, viz., $S_8 = 0.830 \pm 0.016$ [3], than what LSS dynamical probes like weak-lensing, cluster counts, and redshift-space distortion suggest within Λ CDM. For instance, $S_8 = 0.759^{+0.024}_{-0.021}$ (KiDS-1000) [31] and $S_8 = 0.759 \pm 0.025$ (DES-Y3) [32] from low-redshift measurements are in approximately 3σ tension with the Planck- Λ CDM predicted value.

While the scientific community has yet to reach a consensus on whether the H_0 tension arises from systematic errors or yet-to-be-discovered new physics, its persistence across various probes over time diminishes the possibility of systematic causes. This has led many researchers to devote substantial efforts to devising models alternative to Λ CDM. In addressing the H_0 tension, a variety of modifications to Λ CDM have been proposed, which can be broadly categorized as follows: (i) *Early Universe Modifi-*

* anita.math.rs@igu.ac.in

† suresh.kumar@plaksha.edu.in

‡ kibrisc@itu.edu.tr

§ akarsuo@itu.edu.tr

cations: Introducing new physics in the pre-recombination ($z \gtrsim 1100$) universe, essentially to reduce the sound horizon scale and thereby increase the H_0 value. Examples include Early Dark Energy (EDE) [33–38], New EDE [39–41], Anti de-Sitter-EDE [42–44], extra radiation parameterized by the effective number of relativistic species N_{eff} [45–48], combined effects of N_{eff} and EDE [49], and modified gravity [50–56], and oscillations in the inflaton potential [57]. (ii) *Intermediate/Late Universe Modifications*: Introducing new physics at intermediate to late times ($0.1 \lesssim z \lesssim 3.0$) to adjust the expansion history, viz., $H(z)$, aligning H_0 predictions with its local measurements while remaining consistent with CMB and late-time observational data. Examples include the Graduated Dark Energy (gDE) [58], the Λ_s CDM model—mirror Anti de-Sitter to de-Sitter (AdS to dS) transition in the late universe—conjectured from gDE [58–61], the Λ_s VCDM model [62, 63] (VCDM [64, 65] implementation of Λ_s CDM), the Λ_s CDM⁺ model (a stringy model of Λ_s CDM [66–68]), Phantom Crossing Dark Energy [69–75], Omnipotent Dark Energy [69, 74], dynamical DE on top of an AdS background [74, 76–79], (non-minimally) Interacting Dark Energy (IDE) [80–91]¹, running vacuum [93–95], and Phenomenologically Emergent Dark Energy (PEDE) [96]. (iii) *Ultra Late Universe Modifications*: Implementing changes in either fundamental physics or stellar physics during the recent past ($z \lesssim 0.01$) [71, 97–100]. While our list includes some key examples of attempts to resolve the H_0 tension through new physics, it is by no means exhaustive. For a comprehensive overview and detailed classification of various approaches, one may refer to the Refs. [18, 19, 24]. However, addressing the H_0 tension while ensuring compatibility with all available data and without exacerbating other discrepancies, such as the S_8 tension, has turned out to be another challenging task. Currently, only a few models propose simultaneous solutions to both the H_0 and S_8 tensions. Among these, though not exhaustively, are the Λ_s CDM model [58–61], New EDE [40, 41], inflation with oscillations in the inflaton potential [57], some IDE models [84, 86, 91], sterile neutrino with non-zero masses combined with dynamical DE [101], dark matter (DM) with a varying equation of state (EoS) parameter [102], AdS-EDE with ultralight axion [44], some running vacuum models [93, 94]. However, it remains difficult to assert that any model has been widely accepted as both observationally and theoretically fully satisfactory. Among them, the (abrupt) Λ_s CDM model stands out for its simplicity, introducing only one extra free parameter compared to the standard Λ CDM model: z_\dagger , the redshift of the rapid mirror AdS-dS transition. We refer readers to Refs. [69, 74, 76, 78, 79, 103–120]

¹ A recent model-independent reconstruction of the IDE kernel, using Gaussian process methods as suggested in [92], reveals that DE assumes negative densities for $z \gtrsim 2$, suggesting that IDE models do not preclude the possibility of negative DE densities at high redshifts.

for more works considering dark energy assuming negative density values, (mostly) consistent with a negative (AdS-like) cosmological constant, for $z \gtrsim 1.5 - 2$, particularly aiming to address cosmological tensions such as the H_0 and S_8 tensions and, recently, anomalies from JWST. Additionally, Refs. [77, 92, 121–138] suggest such dynamics for dark energy from model-independent/non-parametric observational reconstructions and investigations.

The most popular early-time solutions to the H_0 tension, such as EDE [34, 37, 139, 140] and extra radiation parameterized by the effective number of relativistic species N_{eff} [45–49], involve inserting an additional energy component into the pre-recombination universe to reduce the sound horizon scale, thereby resulting in a higher H_0 [45–48]. However, the extent to which models reducing the sound horizon can tackle the H_0 tension is severely restricted by the fact that they yield a larger matter density ω_m to preserve consistency with the CMB power spectrum, thereby chronically leading to new or worsening some existing discrepancies, such as in the value of S_8 [18–20, 49, 141–143]. Given that early-time modifications focus almost exclusively on the concept of shrinking the sound horizon to increase H_0 , this difficulty in addressing both H_0 and S_8 tensions simultaneously turns an already challenging problem into an even more daunting one from the perspective of early-time solutions.

On the other hand, it is conceivable that a post-recombination extension of the Λ CDM model that addresses the H_0 tension could remain immune to exacerbating the S_8 tension or even address it. A promising candidate is the Λ_s CDM cosmology, inspired by the recent conjecture that the universe underwent a spontaneous mirror AdS-dS transition characterized by a sign-switching cosmological constant (Λ_s) around $z \sim 2$ [58–63]. This conjecture emerged following findings in the gDE model, which demonstrated that a rapid smooth transition from AdS-like DE to dS-like DE at $z \sim 2$ could address the H_0 and BAO Ly- α discrepancies [58]. The Λ_s CDM cosmology involves a sign-switching cosmological constant, a behavior that can typically be described by sigmoid functions, e.g., $\Lambda_s(z) = \Lambda_{s0} \tanh[\eta(z_\dagger - z)] / \tanh[\eta z_\dagger]$, where $\Lambda_{s0} > 0$ is the present-day value of Λ_s and $\eta > 1$ determines the rapidity of the transition; the larger the η , the faster the transition. In the limit as $\eta \rightarrow \infty$, we approach the abrupt Λ_s CDM model [59–63]:

$$\Lambda_s \rightarrow \Lambda_{s0} \operatorname{sgn}[z_\dagger - z] \quad \text{for } \eta \rightarrow \infty, \quad (1)$$

servicing as an idealized depiction of a rapid mirror AdS-dS transition, introducing only one extra free parameter to be constrained by the data, compared to the standard Λ CDM model. To clarify how the abrupt Λ_s CDM model differs from Λ CDM, it is crucial to highlight that, unlike the usual Λ , which remains positive and unchanged throughout cosmic history, $\Lambda_s(z)$ yields a negative value, $\Lambda_s(z) = -\Lambda_{s0}$, for $z > z_\dagger \sim 2$. From physical and mathematical perspectives, this introduces modifications extending from the transition epoch at $z_\dagger \sim 2$ back to the early universe, including the recombination era at $z_{\text{rec}} \sim 1100$

and beyond. In contrast, for $z < z_{\dagger}$, Λ_s CDM becomes identical to Λ CDM, accommodating a positive cosmological constant, $\Lambda_s(z) = \Lambda_{s0}$, after the transition, albeit with a greater value compared to the Λ of Λ CDM, that is $\Lambda_{s0} > \Lambda$, to compensate for its earlier negativity. While this situation suggests an early-time modification from physical and mathematical perspectives, the primary impact of $\Lambda_s(z)$ —its negativity for $z > z_{\dagger} \sim 2$, followed by its transitions to positive values at $z \sim z_{\dagger}$ —is manifested as a deviation in $H(z)$ compared to Λ CDM, but only for $z \lesssim 3$. Specifically, Λ_s CDM predicts a larger expansion rate, $H_{\Lambda_s\text{CDM}}(z) > H_{\Lambda\text{CDM}}(z)$, at low redshifts $z < z_{\dagger}$, and a deformation in $H(z)$ around $z \sim z_{\dagger}$. Therefore, considering the modifications in $H(z)$, from an observational perspective, Λ_s CDM can be regarded as a post-recombination extension of Λ CDM, which could be described as a late-time or moderate-time modification depending on the context. Importantly, at sufficiently high redshifts ($z \gtrsim 3$), the two models become nearly indistinguishable in their dynamics and therefore in observational terms, despite their physical and mathematical differences. This is expected, as the contribution of both Λ_s in Λ_s CDM and Λ in Λ CDM to the total fractional energy density of the Universe is only a few percent by $z \sim 3$, and becomes entirely negligible at even higher redshifts. Particularly, for $3 \lesssim z \lesssim z_{\text{eq}}$ (where $z_{\text{eq}} \sim 3400$ is the redshift of matter-radiation equality), both models effectively reduce to the Einstein-de Sitter universe and reproduce the standard cosmological dynamics prior to recombination (i.e., for $z > z_{\text{rec}} \sim 1100$). Notably, the situation discussed above similarly applies to perturbations, as $\Lambda_s(z)$ affects the linear perturbation and Boltzmann equations solely through the altered late-time expansion rate $H(z)$, without modifying their form. Thus, from physical and mathematical perspectives, Λ CDM is properly recovered from the abrupt Λ_s CDM by sending the transition epoch z_{\dagger} to the limit $z_{\dagger} \rightarrow \infty$. On the other hand, in terms of modifications to the Hubble rate and therefore from an observational perspective, Λ_s CDM is nearly indistinguishable from Λ CDM for $z \gtrsim 3$. This also highlights an important fact: choosing a transition redshift $z_{\dagger} \gtrsim 3$ would make Λ_s CDM practically indistinguishable from Λ CDM in observational terms.

Detailed observational investigations of the Λ_s CDM model suggest that it can simultaneously address the H_0 , M_B , and S_8 tensions, as well as the Ly- α , t_0 , and ω_b anomalies. It is also observed that while the model partially steps back from its achievements when the BAO (3D BAO) dataset is included in the analysis, it remains entirely compatible with the weakly model-dependent transversal BAO, i.e., 2D BAO [59–61]. These phenomenological achievements of Λ_s CDM are now underpinned by significant theoretical progress in elucidating the (mirror) AdS-dS transition phenomenon. The authors of Refs. [66–68] assert that, despite the AdS swampland conjecture suggesting that Λ_s seems unlikely given the AdS and dS vacua are infinitely distant from each other in moduli space, the Casimir energy of fields inhabiting the bulk

can realize the AdS-dS transition conjectured in Λ_s CDM. It was also shown in Refs. [62, 63] that the Λ_s CDM model with this abrupt/rapid transition can effectively be constructed from a particular Lagrangian containing an auxiliary scalar field with a two-segmented linear potential within a type-II minimally modified gravity framework called VCDM [64, 65]

All the aforementioned successes of Λ_s CDM, despite being one of the most minimal deviations from Λ CDM, and the ensuing theoretical developments suggest that missing pieces of the cosmic puzzle, if any, are likely to be identified in the late universe rather than the early universe. Thus, examining both early and late-time modifications within a viable model would be enlightening in our endeavor to restore cosmic concordance. Following this line of reasoning, we investigate the implications of allowing the effective number of neutrino species, N_{eff} , to vary freely along with the redshift at which the mirror AdS-dS transition occurs, z_{\dagger} , in the Λ_s CDM model. The effect of N_{eff} is most pronounced when radiation dominates the universe, while the effect of z_{\dagger} is most noticeable in the late matter-dominated era and beyond. The variation of N_{eff} also provides an excellent avenue to assess how well Λ_s CDM concurs with our best theory of matter, the Standard Model (SM) of particle physics, while addressing major discrepancies like the H_0 and S_8 tensions. In addition to N_{eff} , we relax the minimal mass assumption of Λ CDM and allow the sum of mass eigenstates, $\sum m_{\nu}$, to be a free parameter to test the model’s capabilities and its consistency with neutrino flavor oscillation experiments. Consequently, we place joint constraints on N_{eff} and $\sum m_{\nu}$ in both the Λ_s CDM+ N_{eff} + $\sum m_{\nu}$ and Λ CDM+ N_{eff} + $\sum m_{\nu}$ models. See, e.g., Ref. [144] for a similar investigation conducted in the context of PEDE [96]. We refer readers to Ref. [145] for a comprehensive review on neutrino physics and Refs. [3, 146–162] and references therein for recent discussions and constraints regarding neutrino properties, viz., N_{eff} and $\sum m_{\nu}$, in the context of cosmology.

The remainder of the paper is structured as follows: in Section II, we present the rationale behind this work and explain the underlying physics of the possible outcomes of having a non-standard effective number of relativistic species and neutrino masses. Section III introduces the datasets and elaborates on the methodology utilized in the observational analysis. In Section IV, we present the observational constraints on the model parameters under consideration. We then discuss the results in terms of existing tensions such as the H_0 and S_8 tensions and explore the emergence of new ones like N_{eff} and the resultant Y_p in cases where the data favor large N_{eff} . Finally, we conclude with our main findings in Section V.

II. RATIONALE

In this section, we explore the implications of a two-parameter extension of the abrupt Λ_s CDM model [59–61],

as well as for the Λ CDM model for comparison reasons, achieved by treating N_{eff} and $\sum m_\nu$ as free parameters. Allowing these parameters to vary can significantly impact the early universe and its associated cosmological observables. We detail these effects in the following subsections.

A. Number of relativistic neutrino species

The universe, in its history of evolution, underwent a phase of radiation (r) domination when it was filled with a soup of high energy photons (γ) and other relativistic species, such as electrons (e^-), positrons (e^+), neutrinos (ν), and anti-neutrinos ($\bar{\nu}$). This early universe content can collectively be treated as radiation, and its energy density, ρ_r , can be parameterized in terms of the so-called effective number of relativistic neutrino species, N_{eff} , and the energy density of photons, ρ_γ [163]

$$\rho_r = \rho_\gamma \left[1 + \frac{7}{8} N_{\text{eff}} \left(\frac{4}{11} \right)^{4/3} \right]. \quad (2)$$

In the instantaneous neutrino decoupling limit, the SM of particle physics, which includes three types of active neutrino flavors, suggests $N_{\text{eff}} = 3$. However, in reality, decoupling was an extended process, and neutrinos were not entirely decoupled from the plasma with which they were initially in thermal equilibrium when the e^\pm annihilation began. Consequently, some of the energy and entropy were inevitably transferred from the annihilating e^\pm pairs to neutrinos, particularly to those at high energy tail of the neutrino spectrum, as well as photons, slightly heating and pushing them away from the Fermi-Dirac distribution [164, 165]. Along with QED plasma corrections, the SM therefore predicts the precise value of $N_{\text{eff}} = 3.044$ [166–168]. Any significant departure from this predicted value might hint at either new physics or non-standard neutrino properties. Ascertaining its value in various cosmological models is thus crucial for carrying out a consistency check against known particle physics and for probing the physics beyond.

In this respect, the possibility of the existence of additional relativistic relics, not accommodated by the SM of particle physics, and the absence of a definitive upper bound on $\sum m_\nu$, leave the door open for natural and well-motivated extensions of the six-parameter Λ CDM model. These extensions can be achieved by relaxing N_{eff} and $\sum m_\nu$, either separately or jointly. Considering them as free parameters of the extended models, the *Planck* CMB experiment is capable of constraining N_{eff} through the damping scale and small scale CMB anisotropies (based on the damping tail) [169], which finds $N_{\text{eff}} = 2.92_{-0.38}^{+0.36}$ (95% CL, *Planck* TT,TE,EE+lowE) [3]. Similarly, the sum of neutrino masses $\sum m_\nu$ can be constrained via CMB power spectra and lensing, placing an upper bound of $\sum m_\nu < 0.24$ eV (95% CL, TT,TE,EE+lowE+lensing) [3]. See Ref. [149] for model marginalized constraints on neutrino properties, N_{eff} and $\sum m_\nu$ from various cosmological

data, on top of the standard Λ CDM model and its some well-known extensions. In such models, the effect of dark radiation ρ_{dr} , i.e., extra relativistic degrees of freedom such as sterile neutrinos initially in thermal equilibrium with standard model bath, and any non-standard neutrino behavior, generates a deviation $\Delta N_{\text{eff}} = N_{\text{eff}} - 3.044$ from the SM value $N_{\text{eff}} = 3.044$. If the relic contribution to radiation density is due, say, to extra neutrino species, then we have:

$$\rho_{\text{dr}} = \frac{7}{8} \Delta N_{\text{eff}} \left(\frac{T_\nu}{T_\gamma} \right)^4 \rho_\gamma, \quad (3)$$

where T_γ and T_ν are the temperatures of photons and neutrinos, respectively. When $\Delta N_{\text{eff}} > 0$, the energy density ρ_r in the total radiation content increases since $\rho_r = \rho_{\text{SM}} + \rho_{\text{dr}}$, resulting in an early expansion rate $H(z) = \sqrt{8\pi G \rho_r / 3}$ that is enhanced compared to Λ CDM with ρ_{SM} . One significant consequence of such an enhanced expansion is the reduction of the sound horizon r_* at recombination. To elaborate, the sound horizon is defined as the maximum comoving distance that acoustic waves can travel in photon-baryon plasma, from the beginning of the universe ($z = \infty$) to the last scattering redshift (z_*), and is given by:

$$r_* = \int_{z_*}^{\infty} \frac{c_s(z)}{H(z)} dz, \quad (4)$$

with $c_s(z) = c / \sqrt{3(1 + \frac{3\omega_b}{4\omega_\gamma(1+z)})}$ being the sound speed in the photon-baryon fluid. Here, c is the speed of light in the vacuum, $\omega_b \equiv \Omega_{b,0} h^2$ and $\omega_\gamma \equiv \Omega_{\gamma,0} h^2$ are the physical baryon and photon densities, respectively, with $\Omega_{i,0}$ being the present-day density parameter of the i^{th} fluid and $h = H_0 / 100 \text{ km s}^{-1} \text{ Mpc}^{-1}$ being the reduced Hubble constant. $H(z)$ depends on a given model; therefore, the resultant r_* is also a model-dependent quantity. In Λ CDM, $r_* \sim 144 \text{ Mpc}$ [3]; on the other hand, models with greater early expansion rate $H(z > z_*) > H_{\Lambda\text{CDM}}(z > z_*)$ have correspondingly smaller $r_* < 144 \text{ Mpc}$. Since the sound horizon r_* at decoupling represents a known distance scale, it can be used as a standard ruler to define $D_M(z_*) = r_* / \theta_*$, where:

$$D_M(z_*) = \int_0^{z_*} \frac{c dz}{H(z)} \quad (5)$$

is the comoving angular diameter distance from a present-day observer to the surface of last scattering, and θ_* is the angular acoustic scale. θ_* is very accurately and nearly model-independently measured with a precision of 0.03% according to the spacing of acoustic peaks in the CMB power spectrum, and found to be $100\theta_* = 1.04110 \pm 0.00031$ (*Planck*, 68% CL, TT,TE,EE+lowE+lensing) [3]. This implies that any viable model introducing modifications to $H(z > z_*)$ is expected to keep θ_* fixed at the measured value to remain concordant with the CMB. It then follows that imposing such a condition on θ_* in the case of varying r_* requires $D_M(z_*)$ to change, hence H_0 to

change as well since $D_M(z_*)$ is much less affected by the changing N_{eff} (because the integral Eq. (5) is dominated by its lower limit). That is, for models reducing the sound horizon, H_0 must increase to keep θ_* fixed. In the literature, this is a generic method employed by early-time solutions that modify the pre-recombination universe but leave the post-recombination universe intact, such as EDE models [24, 37], to address the H_0 tension. $\Lambda_s\text{CDM}$, however, with its additional switch parameter z_\dagger , allows for non-standard low redshift evolution as the cosmological constant Λ begins dominating the energy budget in the late universe, which was elaborated in Section I. A negative cosmological constant, $\Lambda < 0$ when $z > z_\dagger$, leads to a reduction in the total energy density relative to that of ΛCDM , resulting in $H_{\Lambda_s\text{CDM}}(z > z_\dagger) < H_{\Lambda\text{CDM}}(z > z_\dagger)$. Besides, both $\Lambda_s\text{CDM}$ and ΛCDM have almost the same sound horizon scale r_* because Λ has a vanishing effect on $H(z)$ at redshifts as high as $z > z_*$, hence effectively the same $r_*/\theta_* = D_M(z_*)$. The deficit in $H_{\Lambda_s\text{CDM}}(z > z_\dagger)$ prior to the switching must then be compensated by an enhanced $H_{\Lambda_s\text{CDM}}(z < z_\dagger)$, implying a larger H_0 , since the $D_M(z_*)$ integrals in both models must yield the same result. We note in this regard that the $\Lambda_s\text{CDM} + N_{\text{eff}} + \sum m_\nu$ model represents a scenario accommodating both early (N_{eff}) and late (z_\dagger) time degrees of freedom, which can be constrained by observational data. Confrontation of such models with observational data might provide extremely valuable hints as to whether we should seek physics/modifications beyond/in the standard model of cosmology in the early or late universe, or both (see Refs. [20, 21] for a further discussion). $\Lambda_s\text{CDM} + N_{\text{eff}} + \sum m_\nu$ would therefore serve as a very illuminating and powerful guide in the quest to develop a more complete and observationally consistent cosmological framework.

B. Sum of Neutrino Masses

It was long assumed in the SM of particle physics that neutrinos were massless family of leptons. However, confirmed by atmospheric and solar neutrino observations, they have been found to have non-zero, albeit very small, masses [170]. In this sense, what can be considered as a first step beyond the SM has come not from N_{eff} measurements but from efforts to determine neutrino masses. Although their exact masses have not been pinpointed yet, we know that at least two of their mass states are massive, and neutrino oscillation experiments can place bounds on the so-called mass splittings $\Delta m_{ij}^2 = m_i^2 - m_j^2$, where $i, j = 1, 2, 3$ label mass eigenstates m_i and m_j belonging to different neutrino types. Cosmological observations are sensitive to the sum of neutrino masses $\sum m_\nu$, which in the normal hierarchy (NH) $m_1 \ll m_2 < m_3$, is given by $\sum m_\nu = m_0 + \sqrt{\Delta m_{21}^2 + m_0^2} + \sqrt{|\Delta m_{31}|^2 + m_0^2}$, where m_0 is the lightest neutrino mass and conventionally $m_0 \equiv m_1$ in the normal mass ordering [170]. Taking the lightest neutrino mass to be zero ($m_1 = 0$), we can

use the oscillation data, $\Delta m_{21}^2 = 7.49_{-0.17}^{+0.29} \times 10^{-5} \text{ eV}^2$ and $\Delta m_{31}^2 = 2.484_{-0.048}^{+0.045} \times 10^{-3} \text{ eV}^2$, to compute the minimal sum of masses and find the lower bound $\sum m_\nu \sim 0.06 \text{ eV}$ [171]. Performing the same calculation for the inverted hierarchy (IH) with $m_3 \ll m_1 < m_2$ yields $\sum m_\nu \sim 0.1 \text{ eV}$. Thus, any total mass value $\sum m_\nu < 0.06 \text{ eV}$ is ruled out by the oscillation experiments. ΛCDM assumes the normal mass hierarchy with the minimal mass $\sum m_\nu = 0.06 \text{ eV}$ [3]; however, unless they are in conflict with observations, there is no well-justified theoretical underpinning for why neutrinos with reasonably greater mass values should not be considered in a given cosmological model. See Ref. [149] for model marginalized constraints on neutrino properties, N_{eff} and $\sum m_\nu$ from cosmology, on top of the standard ΛCDM model and its some well-known extensions. Provided that neutrinos are not so massive, that is $\sum m_\nu < 1 \text{ eV}$, they are relativistic prior to recombination, behaving like radiation. After around the time of recombination, they transition from being radiation-like particles to being matter-like particles. Although massive neutrinos increase the physical density of matter ω_m by an amount of about $\omega_\nu \approx \sum m_\nu / 93 \text{ eV}$, at small scales they tend to erase the growth of gravitational potential wells created by CDM due to their high thermal speed. In other words, unlike CDM, they do not cluster on scales smaller than their free-streaming length, which leads to the suppression of the (late time) clustering amplitude σ_8 , hence to the suppression of the growth factor $S_8 = \sigma_8 \sqrt{\Omega_m / 0.3}$ [172]. Such a feature might render massive neutrinos an effective tool in tackling the S_8 tension, especially in potential situations where pre-recombination expansion rate is hastened by a non-negligible amount of extra radiation, namely $\Delta N_{\text{eff}} > 0$. This additional species causes a magnified early integrated Sachs-Wolfe effect that manifests itself as an enhancement in the heights of the first two CMB acoustic peaks (most noticeable at $\ell \sim 200$). In order for the fit to the CMB power spectrum that is already outstanding in the baseline ΛCDM not to deteriorate, this excess power at low- ℓ can be offset by an accompanying increase in ω_m , the impact of which is to eventually worsen the so-called S_8 tension. On the other hand, the degree to which massive neutrinos can actually counteract the effect of ω_m -induced power is limited by the H_0 tension because large $\sum m_\nu$ values shrink the comoving angular diameter distance to the last scattering surface given by Eq. (5), shifting the acoustic peaks to low- ℓ . The fit can then simply be restored by lowering H_0 . Note that this signals a strong degeneracy between H_0 and $\sum m_\nu$, meaning large $\sum m_\nu$ values that are supposed to suppress S_8 act to aggravate the H_0 tension, which lends further support to the view that the simultaneous elimination of H_0 and S_8 tensions is a formidable task, particularly for models enhancing the pre-recombination expansion rate as early-time solutions (for a list of early-time solution suggestions, see Ref. [19]).

C. Primordial Helium Abundance

The abundance of light elements, particularly helium, is proportional to N_{eff} as the early expansion rate $H(z)$ directly affects the rate of Big Bang Nucleosynthesis (BBN). To understand this, consider the interaction rate per particle, $\Gamma = n_\nu \langle \sigma v \rangle$, where n_ν is the number density of neutrinos, $\langle \sigma v \rangle$ is the thermally-averaged cross-section of the weak interaction, and v is the relative particle speed. The amount of helium formed in the first few minutes of the universe is determined by two competing factors: $H(z)$ and $\Gamma(z)$. As long as $\Gamma \gg H$, neutrons and protons maintain chemical equilibrium via weak interactions. As the temperature drops below $T \sim 1$ MeV with expansion, the weak interaction loses efficiency, causing neutrons to go out of equilibrium and freeze the neutron-proton ratio, n_n/n_p , at the freeze-out temperature T_f . We can determine T_f using the relation $\Gamma = n_\nu \langle \sigma v \rangle \sim G_F^2 T^5$, as $n_\nu \sim T^3$ and $\langle \sigma v \rangle \sim G_F^2 T^2$, where $G_F = 1.166 \times 10^{-5} \text{ GeV}^{-2}$ is the Fermi coupling constant. In the early universe, dominated by radiation, the Friedmann equation can be expressed as

$$H = \sqrt{\frac{4\pi^3}{45 m_{\text{Pl}}^2} g_* T^4}, \quad (6)$$

where $m_{\text{Pl}} = G^{-1/2} = 1.22 \times 10^{19} \text{ GeV}$ is the Planck mass scale, and g_* represents the effective number of degrees of freedom internal to each particle. Neutrons freeze out approximately when $\Gamma(T_f) \approx H(T_f)$, which implies:

$$T_f \sim \left(\frac{\sqrt{g_*}}{G_F^2 m_{\text{Pl}}} \right)^{1/3}. \quad (7)$$

Injecting extra relativistic degrees of freedom with $\Delta N_{\text{eff}} > 0$ results in a higher g_* . If the relic is a fermion, g_* is adjusted as follows:

$$g_* = g_{*\text{SM}} + \frac{7}{8} g_{\text{rel}} \left(\frac{T_{\text{rel}}}{T_\gamma} \right)^4, \quad (8)$$

leading to enhanced expansion rate as $H \propto \sqrt{g_*} T^2$. Consequently, T_f increases as it is proportional to $g_*^{1/6}$ [173]. The neutron fraction in equilibrium,

$$\frac{n_n}{n_p} = e^{-\Delta m/T_f}, \quad (9)$$

where $\Delta m = m_n - m_p = 1.293 \text{ MeV}$ is the mass difference between neutron and proton, dictates that at higher temperatures of T_f , neutrons not only freeze out sooner than in the standard case but also in larger numbers. While a portion of these neutrons undergo spontaneous β^- decay, most end up in He^4 nuclei, leading to increased helium production compared to the standard BBN. Using the neutron fraction $n_n/n_p \sim 1/7$, we can roughly estimate the primordial helium-4 mass fraction Y_p :

$$Y_p = \frac{2(n_n/n_p)}{1 + (n_n/n_p)} \approx 0.25. \quad (10)$$

The modification of Y_p due to $\Delta N_{\text{eff}} \neq 0$ can be approximated by $\Delta Y_p \approx 0.013 \times \Delta N_{\text{eff}}$ [174]. Thus, a model with a sufficiently large $\Delta N_{\text{eff}} > 0$ could easily overestimate Y_p , limiting the scope for significant variations in N_{eff} .

III. DATASETS AND METHODOLOGY

To constrain the model parameters, we utilize multiple datasets, including the Planck CMB, BAO, BAOtr, and PantheonPlus&SH0ES.

- *CMB*: The CMB data was obtained from the Planck 2018 legacy data release, a comprehensive dataset widely recognized for its precision and accuracy. Our analysis incorporated CMB temperature anisotropy and polarization power spectra measurements, their cross-spectra, and lensing power spectrum [175, 176]. This analysis utilizes the high- ℓ *Planck* likelihood for TT (where $30 \leq \ell \leq 2508$), as well as TE and EE (where $30 \leq \ell \leq 1996$). Additionally, it incorporates the low- ℓ TT-only likelihood (where $2 \leq \ell \leq 29$) based on the *Commander* component-separation algorithm in pixel space, the low- ℓ EE-only likelihood (where $2 \leq \ell \leq 29$) using the *SimAll* method, and measurements of the CMB lensing. This dataset is conveniently referred to as *Planck*.

- *BAO*: We utilize 14 Baryon Acoustic Oscillation (BAO) measurements, which consist of both isotropic and anisotropic BAO measurements. The isotropic BAO measurements are identified as $D_V(z)/r_d$, where $D_V(z)$ characterizes the spherically averaged volume distance, and r_d represents the sound horizon at the baryon drag epoch. The anisotropic BAO measurements encompass $D_M(z)/r_d$ and $D_H(z)/r_d$, with $D_M(z)$ denoting the comoving angular diameter distance and $D_H(z) = c/H(z)$ indicating the Hubble distance. These measurements have been derived from extensive observations conducted by the Sloan Digital Sky Survey (SDSS) collaboration. These measurements, which span eight distinct redshift intervals, have been acquired and continuously refined over the past 20 years [6]. This dataset is conveniently referred to as *BAO*.²

² *BAO* here refers to the widely used standard 3D BAO data, which are inherently sensitive to the combination $H_0 r_d$, where r_d (the sound horizon at the drag epoch) is primarily determined by the pre-recombination physics of the universe. Consequently, achieving higher values of H_0 compared to the Planck- Λ CDM baseline requires modifications to r_d , which in turn necessitates introducing new physics prior to recombination [177–187], as exemplified by EDE models [33–44]. This dependence strongly suggests that resolving the H_0 tension solely through late-time, post-recombination physics and/or $H(z)$ deformations is challenging, if not impossible. Such models are inherently incapable of modifying r_d and, as a result, tend to degrade the fit to 3D BAO data, which imposes stringent constraints on the expansion rate normalization at $z \lesssim 2$. This limitation, however, may not apply—or is at least considerably diminished—when considering 2D BAO data—also known as Transversal BAO (BAOtr); see the next item, *Transversal BAO*, and Refs. [61, 67, 91, 116, 119, 188–201] for

• *Transversal BAO*: The dataset comprises measurements of the BAO in 2D, specifically referred to as $\theta_{\text{BAO}}(z)$. These measurements are obtained using a weakly model-dependent approach and are compiled in Table I in [192, 194]. The dataset originates from various public data releases (DR) of the SDSS, which includes DR7, DR10, DR11, DR12, DR12Q (quasars), and consistently follows the same methodology across these releases. It is noteworthy that these transversal BAO measurements tend to exhibit larger errors compared to those derived using a fiducial cosmology. This discrepancy arises because the error in the Transversal BAO methodology is determined by the magnitude of the BAO bump, whereas the fiducial cosmology approach, which is model-dependent, yields smaller errors. Generally, the error in the former approach can vary from approximately 10% to as much as 18%, while the latter approach typically results in errors on the order of a few percent [206]. Furthermore, a notable feature of this 2D BAO dataset is the absence of correlations between measurements at different redshifts. This absence of correlation is a result of the methodology employed, which ensures that measurements are derived from cosmic objects within separate redshift shells, preventing correlation between adjacent data bins. See also Footnote 2 for additional context. This dataset is conveniently referred to as *BAOtr*.

• *Type Ia supernovae and Cepheids*: In the likelihood function, we integrate distance modulus measurements of Type Ia supernovae extracted from the Pantheon+ sample [207], incorporating the latest SH0ES Cepheid host distance anchors [25]. The PantheonPlus dataset encompasses 1701 light curves associated with 1550 distinct SNe Ia events, spanning the redshift range $z \in [0.001, 2.26]$. This amalgamated dataset is conveniently denoted as

examples of discussions on these data and their use in obtaining cosmological constraints. Unlike their 3D counterparts, BAOtr data—which primarily probe the angular clustering of galaxies—are argued to exhibit less dependence on the fiducial cosmology. The standard BAO analysis requires converting angular positions and redshifts into Cartesian coordinates to calculate clustering statistics, a process that necessitates adopting a fiducial cosmology. Typically, this fiducial model is assumed to be the base Λ CDM model with parameters constrained by Planck-CMB data. Although this approach accounts for the fiducial assumptions by incorporating geometric scaling parameters, existing studies with alternative models—such as w CDM, EDE, and Horndeski models of modified gravity—have not identified significant biases in 3D BAO analyses due to the choice of fiducial cosmology [202–205]. However, these investigations generally do not explore scenarios involving substantial deviations from Planck- Λ CDM’s late-time dynamics, such as those proposed in Λ_s CDM, where a rapid mirror AdS-to-dS transition occurs in the late universe, namely, around $z \sim 2$. Evaluating whether the standard 3D BAO analysis introduces biases under such conditions would require generating 3D BAO data directly using Λ_s CDM as the fiducial cosmology—a task yet to be undertaken, but one that could yield critical insights. Meanwhile, to ensure a robust assessment, our analysis incorporates both the conventional 3D BAO data, representing a conservative approach, and the less conventional BAOtr data, which are argued to carry less cosmological model dependence.

PantheonPlus&SH0ES.

In the context of the Λ_s CDM+ $N_{\text{eff}}+\sum m_\nu$ model, the baseline comprises nine free parameters represented as $\mathcal{P} = \{\omega_b, \omega_c, \theta_s, A_s, n_s, \tau_{\text{reio}}, N_{\text{eff}}, \sum m_\nu, z_\dagger\}$, with the first eight parameters being identical to those of the Λ CDM+ $N_{\text{eff}}+\sum m_\nu$ model. Throughout our statistical analyses, we adopt flat priors for all parameters: $\omega_b \in [0.018, 0.024]$, $\omega_c \in [0.10, 0.14]$, $100 \theta_s \in [1.03, 1.05]$, $\ln(10^{10} A_s) \in [3.0, 3.18]$, $n_s \in [0.9, 1.1]$, $\tau_{\text{reio}} \in [0.04, 0.125]$, $N_{\text{eff}} \in [0, 5]$, $\sum m_\nu \in [0, 1]$, and $z_\dagger \in [1, 3]$.³

We employ Monte Carlo Markov Chain (MCMC) techniques to sample the posterior distributions of the model’s parameters by using publicly available CLASS+MontePython code [209–211] for different combinations of datasets considered in our analysis. To ensure the convergence of our MCMC chains, we have used the Gelman-Rubin criterion $R - 1 < 0.01$ [212]. We have also made use of the GetDist Python package to perform an analysis of the samples. In the last row of Table I, for the model comparison, we calculate the relative log-Bayesian evidence ($\ln B_{ij}$) using the publicly accessible MCEvidence package⁴ [213, 214] to approximate the Bayesian evidence of extended Λ_s CDM model relative to the extended Λ CDM model. We follow the convention of indicating a negative value when the Λ_s CDM+ $N_{\text{eff}}+\sum m_\nu$ model is favored over the Λ CDM+ $N_{\text{eff}}+\sum m_\nu$ scenario, or vice versa. For the purpose of interpreting the findings, we make use of the updated Jeffrey’s scale introduced by Trotta [215, 216]. We classify the evidence’s strength as follows: it is considered inconclusive when $0 \leq |\ln B_{ij}| < 1$, weak if $1 \leq |\ln B_{ij}| < 2.5$, moderate if $2.5 \leq |\ln B_{ij}| < 5$, strong if $5 \leq |\ln B_{ij}| < 10$, and very

³ It is worth noting that the prior range for z_\dagger used in our analysis follows the one established in the literature [59–61, 63]. Considering the values of $\Omega_m h^2$ and $D_M(z_*)$ fixed by the Planck-CMB spectra, at $z \approx 1.2$, the negative $\Lambda_s(z > z_\dagger)$ would dominate the matter content, causing the universe to start contracting before transitioning to the positive $\Lambda_s(z < z_\dagger)$ phase [59] could occur. Allowing $z_\dagger = 1$ accounts even for this extreme possibility, and it is known that a Planck-CMB-alone analysis readily yields a lower bound of $z_\dagger > 1.45$ at the 95% CL. On the other hand, for $z_\dagger = 3$, the values of H_0 and Ω_m match the Planck- Λ CDM predictions. Therefore, the z_\dagger prior range we considered effectively encompasses the Λ CDM limit from the perspective of observational data analysis. Indeed, it has been shown in Ref. [208] that the constraints on the parameters of a Λ_s CDM model, which also allows for pre-combination universe modifications (via varying electron mass), as considered in the present study, are not affected by the choice of a broader prior range $z_\dagger \in [1, 3.5]$, by introducing a larger upper prior limit of $z_\dagger = 3.5$. For further details, see, for instance, Fig. 2 in Ref. [59] for the case of H_0 versus z_\dagger , as well as the discussion following Eq. (1) in Section I of the current paper. Additionally, it is well known that overly broad prior ranges for parameters penalize models in Bayesian evidence calculations. To mitigate this, we have selected appropriate prior ranges for z_\dagger , as well as for the other free parameters, ensuring also that the constraints are not unduly influenced by prior dominance. This allows us to derive meaningful parameter constraints while conducting a robust and unbiased Bayesian evidence analysis.

⁴ github.com/yabebalFantaye/MCEvidence

strong if $|\ln B_{ij}| \geq 10$.

IV. RESULTS AND DISCUSSION

We present in Table I the marginalized constraints at a 68% confidence level (CL) on various parameters of the extended (abrupt) Λ_s CDM and Λ CDM models, namely, the (abrupt) Λ_s CDM+ N_{eff} + $\sum m_\nu$ and Λ CDM+ N_{eff} + $\sum m_\nu$, utilizing various combinations of datasets including *Planck*, *Planck+BAO*, *Planck+BAOtr*, *Planck+BAO+PP&SH0ES*, and *Planck+BAOtr+PP&SH0ES*. The table also includes the relative log-Bayesian evidence ($\ln B_{ij}$), where a negative value indicates a preference for the Λ_s CDM+ N_{eff} + $\sum m_\nu$ model over the Λ CDM+ N_{eff} + $\sum m_\nu$. In the current study, for the first time, we constrain the parameters N_{eff} and $\sum m_\nu$ within the framework of the Λ_s CDM cosmology, employing the combinations of datasets in our analysis. As N_{eff} and $\sum m_\nu$ are treated as free parameters in the current study, the errors associated with the constraints are increased compared to those of the base (abrupt) Λ_s CDM and Λ CDM models, considering the same combinations of datasets presented in Refs. [59, 61, 63].⁵ The analysis of CMB-alone data yields $N_{\text{eff}} = 2.91 \pm 0.19$ and $H_0 = 69.00^{+2.10}_{-3.70} \text{ km s}^{-1} \text{ Mpc}^{-1}$ for the Λ_s CDM+ N_{eff} + $\sum m_\nu$ model, while the Λ CDM+ N_{eff} + $\sum m_\nu$ model results in $N_{\text{eff}} = 2.88 \pm 0.18$ and $H_0 = 65.50^{+2.00}_{-1.60} \text{ km s}^{-1} \text{ Mpc}^{-1}$. These values are in close alignment with their Planck-alone constraints in the base models, showing only 0.5σ deviation from $H_0 = 70.77^{+0.79}_{-2.70} \text{ km s}^{-1} \text{ Mpc}^{-1}$ for Λ_s CDM and a 1.0σ deviation from $H_0 = 67.39 \pm 0.55 \text{ km s}^{-1} \text{ Mpc}^{-1}$ for Λ CDM [63]. Notably, both extended models exhibit reduced mean values of H_0 relative to their base counterparts, with broader uncertainties. This effect is more pronounced in the extended Λ CDM model, largely reflecting the reduced mean values and increased error margins of N_{eff} compared to the standard value of $N_{\text{eff}} = 3.044$. Consequently, when compared with the SH0ES measurement of $H_0 = 73.04 \pm 1.04 \text{ km s}^{-1} \text{ Mpc}^{-1}$ [25], the H_0 tension is significantly alleviated to 1.3σ for the Λ_s CDM+ N_{eff} + $\sum m_\nu$ model, whereas it reduces only to 3.6σ for the Λ CDM+ N_{eff} + $\sum m_\nu$ model. The predicted N_{eff} values are consistent with the SM value of $N_{\text{eff}} = 3.044$ [166–168] within 1σ for both models. The models yield similar constraints on the total neutrino mass, with $\sum m_\nu < 0.41 \text{ eV}$ at a 95% CL for the

Λ_s CDM+ N_{eff} + $\sum m_\nu$ model and $\sum m_\nu < 0.40 \text{ eV}$ at a 95% CL for the Λ CDM+ N_{eff} + $\sum m_\nu$ model. The parameter z_\dagger in the Λ_s CDM+ N_{eff} + $\sum m_\nu$ model remains unconstrained, while in the base Λ_s CDM model, it establishes a lower bound of $z_\dagger > 1.45$ at 95% CL.

We also present in Figs. 1 and 2 the one- and two-dimensional marginalized distributions of the extended Λ_s CDM and Λ CDM model parameters at 68% and 95% CL for the Planck, Planck+BAO/BAOtr, and Planck+BAO/BAOtr+PP&SH0ES datasets. We observe a strong positive correlation between H_0 and N_{eff} owing to the physical mechanism discussed in Section II A. Notably, the addition of data from low redshift probes such as BAO/BAOtr and supernova samples, which fix the late-universe evolution, helps break the geometric degeneracies and tighten the constraints on N_{eff} and other related parameters. With that being said, all the datasets that favor somewhat large H_0 values, with $H_0 \gtrsim 70 \text{ km s}^{-1} \text{ Mpc}^{-1}$, also show preference for a relatively significant deviation from $N_{\text{eff}} = 3.044$, except for the Λ_s CDM + N_{eff} + $\sum m_\nu$ model when subjected to Planck+BAOtr and Planck+BAOtr+PP&SH0ES, which warrants particular attention. In these datasets, the extended Λ_s CDM model yields H_0 values in excellent agreement with the SH0ES measurement, specifically $H_0 = 73.10 \pm 1.40 \text{ km s}^{-1} \text{ Mpc}^{-1}$ and $H_0 = 73.08 \pm 0.76 \text{ km s}^{-1} \text{ Mpc}^{-1}$, respectively. Similarly, the extended Λ CDM model provides $H_0 = 70.10 \pm 1.30 \text{ km s}^{-1} \text{ Mpc}^{-1}$ and $H_0 = 72.23 \pm 0.74 \text{ km s}^{-1} \text{ Mpc}^{-1}$, respectively, both aligning well with SH0ES measurement. However, when compared to their base models, the extended Λ_s CDM remains closely aligned with the base Λ_s CDM results, showing only a 0.1σ deviation with $H_0 = 73.30^{+1.20}_{-1.00} \text{ km s}^{-1} \text{ Mpc}^{-1}$ and a 0.3σ deviation with $H_0 = 72.82 \pm 0.65 \text{ km s}^{-1} \text{ Mpc}^{-1}$ [61]. In contrast, the extended Λ CDM model shows some tension with the base Λ CDM model values, with deviations of 0.9σ and 3.1σ for $H_0 = 68.84 \pm 0.48 \text{ km s}^{-1} \text{ Mpc}^{-1}$ and $H_0 = 69.57 \pm 0.42 \text{ km s}^{-1} \text{ Mpc}^{-1}$, respectively [61]. This stability in the Λ_s CDM framework, absent in the Λ CDM framework, reflects the fact that the extended Λ_s CDM model's predictions for N_{eff} and $\sum m_\nu$ are consistent with standard neutrino properties, thereby maintaining close agreement with the base Λ_s CDM model. Importantly, in the Λ_s CDM + N_{eff} + $\sum m_\nu$ model H_0 values that agree well with the ones measured using the local distance ladder approach can be realized in two ways: either by shrinking the sound horizon scale r_* due to the introduction of extra relics to the early universe, i.e., $\Delta N_{\text{eff}} > 0$, while keeping the sign switch redshift z_\dagger at large enough values where the model is not significantly distinguishable from its Λ CDM counterpart, or by adhering approximately to the standard value of neutrino species ($\Delta N_{\text{eff}} \sim 0$) and allowing a value of $z_\dagger \sim 2$, resulting in a significantly larger H_0 due to the abrupt mirror AdS-dS transition in the late universe as discussed above. We read off from Table I that Planck+BAOtr and Planck+BAOtr+PP&SH0ES favor exactly the latter case by placing the constraints $N_{\text{eff}} = 2.97 \pm 0.19$ and

⁵ We note that the BAO dataset used in [63] includes an additional data point, specifically DES Y6 BAO, compared to the dataset used here, which follows [59]. However, a comparison of the CMB+BAO constraints on the base models in Refs. [59] and [63] reveals no significant change in the constraints. Therefore, this one data point difference between these BAO datasets does not significantly impact our results and can be considered equivalent for the purposes of the comparative discussions below.

TABLE I. Marginalized constraints, mean values with 68% CL, on the free and some derived parameters of the $\Lambda_s\text{CDM}+N_{\text{eff}}+\sum m_\nu$ and $\Lambda\text{CDM}+N_{\text{eff}}+\sum m_\nu$ models for different dataset combinations. The relative log-Bayesian evidence given by $\ln \mathcal{B}_{ij} = \ln \mathcal{Z}_{\Lambda\text{CDM}+N_{\text{eff}}+\sum m_\nu} - \ln \mathcal{Z}_{\Lambda_s\text{CDM}+N_{\text{eff}}+\sum m_\nu}$ are also displayed in the last row for the different analyses so that a negative value indicates a preference for the $\Lambda_s\text{CDM}+N_{\text{eff}}+\sum m_\nu$ model over the $\Lambda\text{CDM}+N_{\text{eff}}+\sum m_\nu$ scenario. The parameter $\sum m_\nu$ shows upper bound of 95% CL.

Dataset	Planck	Planck+BAO	Planck+BAOtr	Planck+BAO +PP&SH0ES	Planck+BAOtr +PP&SH0ES
Model	$\Lambda_s\text{CDM}+N_{\text{eff}}+\sum m_\nu$	$\Lambda_s\text{CDM}+N_{\text{eff}}+\sum m_\nu$	$\Lambda_s\text{CDM}+N_{\text{eff}}+\sum m_\nu$	$\Lambda_s\text{CDM}+N_{\text{eff}}+\sum m_\nu$	$\Lambda_s\text{CDM}+N_{\text{eff}}+\sum m_\nu$
	$\Lambda\text{CDM}+N_{\text{eff}}+\sum m_\nu$	$\Lambda\text{CDM}+N_{\text{eff}}+\sum m_\nu$	$\Lambda\text{CDM}+N_{\text{eff}}+\sum m_\nu$	$\Lambda\text{CDM}+N_{\text{eff}}+\sum m_\nu$	$\Lambda\text{CDM}+N_{\text{eff}}+\sum m_\nu$
$10^2\omega_b$	2.227 ± 0.023 2.218 ± 0.022	2.218 ± 0.019 2.234 ± 0.018	2.239 ± 0.021 $2.272^{+0.019}_{-0.022}$	2.264 ± 0.016 2.282 ± 0.015	$2.247^{+0.017}_{-0.023}$ $2.298^{+0.013}_{-0.015}$
ω_{cdm}	0.1181 ± 0.0029 0.1183 ± 0.0029	0.1179 ± 0.0030 $0.1179^{+0.0026}_{-0.0029}$	0.1179 ± 0.0029 0.1188 ± 0.0030	0.1263 ± 0.0025 0.1262 ± 0.0024	0.1205 ± 0.0023 0.1239 ± 0.0026
$100\theta_s$	1.04220 ± 0.00050 1.04221 ± 0.00052	1.04224 ± 0.00051 1.04219 ± 0.00051	1.04211 ± 0.00051 $1.04192^{+0.00046}_{-0.00053}$	1.04105 ± 0.00042 1.04097 ± 0.00040	1.04181 ± 0.00043 1.04119 ± 0.00041
$\ln(10^{10}A_s)$	3.037 ± 0.017 3.038 ± 0.018	3.035 ± 0.018 $3.041^{+0.014}_{-0.017}$	3.035 ± 0.017 3.062 ± 0.018	3.061 ± 0.017 $3.067^{+0.014}_{-0.017}$	3.044 ± 0.018 3.076 ± 0.015
n_s	0.9609 ± 0.0088 $0.9576^{+0.0086}_{-0.0075}$	0.9575 ± 0.0076 0.9628 ± 0.0069	0.9659 ± 0.0082 0.9777 ± 0.0076	$0.9776^{+0.0056}_{-0.0062}$ 0.9835 ± 0.0053	0.9696 ± 0.0076 0.9891 ± 0.0049
τ_{reio}	0.0534 ± 0.0076 0.0532 ± 0.0078	0.0529 ± 0.0076 $0.0554^{+0.0063}_{-0.0077}$	0.0524 ± 0.0074 0.0634 ± 0.0084	0.0554 ± 0.0079 $0.0583^{+0.0067}_{-0.0082}$	0.0546 ± 0.0080 $0.0645^{+0.0073}_{-0.0083}$
z_{\dagger}	unconstrained	> 1.69 (95% CL)	$1.57^{+0.16}_{-0.22}$	> 1.65 (95% CL)	$1.62^{+0.19}_{-0.30}$
N_{eff}	— 2.91 ± 0.19 2.88 ± 0.18	— 2.87 ± 0.19 $2.93^{+0.16}_{-0.18}$	— 2.97 ± 0.19 3.17 ± 0.19	— 3.44 ± 0.15 3.50 ± 0.13	— $3.11^{+0.13}_{-0.15}$ 3.50 ± 0.13
$\sum m_\nu$ [eV]	< 0.41 < 0.40	< 0.41 < 0.13	< 0.35 < 0.06	< 0.48 < 0.13	< 0.49 < 0.06
H_0 [km/s/Mpc]	$69.00^{+2.10}_{-3.70}$ $65.50^{+2.00}_{-1.60}$	67.20 ± 1.20 67.10 ± 1.10	73.10 ± 1.40 70.10 ± 1.30	$71.09^{+0.81}_{-0.70}$ 70.95 ± 0.75	73.08 ± 0.76 72.23 ± 0.74
M_B [mag]	— —	— —	— —	$-19.329^{+0.024}_{-0.019}$ -19.334 ± 0.022	-19.281 ± 0.021 -19.302 ± 0.021
Ω_m	$0.3000^{+0.0290}_{-0.0240}$ $0.3310^{+0.0120}_{-0.0230}$	0.3150 ± 0.0087 0.3128 ± 0.0072	0.2654 ± 0.0085 0.2885 ± 0.0079	0.2996 ± 0.0069 0.2970 ± 0.0055	0.2713 ± 0.0066 $0.2819^{+0.0048}_{-0.0054}$
σ_8	$0.793^{+0.030}_{-0.021}$ $0.790^{+0.030}_{-0.015}$	$0.781^{+0.023}_{-0.017}$ $0.809^{+0.012}_{-0.010}$	$0.812^{+0.022}_{-0.014}$ 0.822 ± 0.011	$0.802^{+0.025}_{-0.019}$ $0.834^{+0.011}_{-0.009}$	$0.811^{+0.028}_{-0.013}$ 0.837 ± 0.009
S_8	$0.792^{+0.029}_{-0.016}$ 0.830 ± 0.013	$0.800^{+0.018}_{-0.013}$ $0.825^{+0.012}_{-0.010}$	$0.763^{+0.019}_{-0.014}$ 0.806 ± 0.012	$0.801^{+0.020}_{-0.015}$ 0.830 ± 0.011	$0.771^{+0.022}_{-0.014}$ 0.811 ± 0.012
Y_p	0.2461 ± 0.0026 0.2456 ± 0.0026	0.2454 ± 0.0026 0.2464 ± 0.0024	0.2470 ± 0.0026 0.2497 ± 0.0025	0.2532 ± 0.0020 0.2541 ± 0.0017	0.2489 ± 0.0020 0.2542 ± 0.0017
z_d	$1059.52^{+0.73}_{-0.82}$ 1059.26 ± 0.74	1059.29 ± 0.71 1059.60 ± 0.74	1059.88 ± 0.82 1060.82 ± 0.72	1061.42 ± 0.55 1061.82 ± 0.50	1060.34 ± 0.58 1061.99 ± 0.49
r_d [Mpc]	148.3 ± 1.9 148.5 ± 1.8	148.7 ± 1.9 148.3 ± 1.7	147.9 ± 1.8 146.4 ± 1.8	143.1 ± 1.4 142.8 ± 1.2	146.4 ± 1.4 143.2 ± 1.3
z_*	1085.17 ± 0.85 1085.22 ± 0.86	1085.29 ± 0.81 1084.86 ± 0.75	1085.08 ± 0.83 1084.00 ± 0.88	1085.78 ± 0.82 1085.30 ± 0.81	1085.32 ± 0.78 1084.30 ± 0.92
r_* [Mpc]	146.1 ± 1.8 146.4 ± 1.8	146.4 ± 1.7 146.2 ± 1.8	145.6 ± 2.0 144.2 ± 1.7	141.1 ± 1.4 140.7 ± 1.2	144.2 ± 1.4 141.3 ± 1.2
χ^2_{min}	2777.98 2777.22	2787.52 2787.36	2793.62 2815.36	4101.96 4104.24	4096.86 4118.56
$\ln \mathcal{Z}$	-1425.54 -1426.17	-1431.99 -1433.97	-1434.83 -1446.56	-2088.61 -2089.85	-2087.11 -2098.16
$\ln \mathcal{B}_{ij}$	-0.63	-1.98	-11.73	-1.24	-11.05

$N_{\text{eff}} = 3.11_{-0.15}^{+0.13}$, respectively, well consistent with the standard particle physics value of $N_{\text{eff}} = 3.044$ [166–168]. The strong degeneracy of characteristic parameter z_{\dagger} of the Λ_s CDM model is broken and it is constrained to be $z_{\dagger} = 1.57_{-0.22}^{+0.16}$ and $z_{\dagger} = 1.62_{-0.30}^{+0.19}$, corresponding to time periods when the dark energy density is non-negligible and therefore Λ_s CDM + $N_{\text{eff}} + \sum m_{\nu}$ is statistically distinct from Λ CDM + $N_{\text{eff}} + \sum m_{\nu}$. Notably, the transition redshifts obtained here are in complete agreement with those for the base Λ_s CDM model, with values of $z_{\dagger} = 1.70_{-0.19}^{+0.09}$ (deviation of only 0.6σ) and $z_{\dagger} = 1.70_{-0.13}^{+0.10}$ (deviation of only 0.3σ) [61]. The upshot is that the observational data do not spoil the early universe account of the SM, keeping N_{eff}, r_*, r_d , and Y_p at values comparable to those in the standard Λ CDM model as shown in Figs. 3 and 4, but instead call for new physics or modification in the post-recombination universe.

Moreover, it is noteworthy that replacement of BAOtr dataset with BAO holds back both models from attaining H_0 values consistent with SH0ES measurements, thereby from efficiently resolving the H_0 tension. Notice also that inclusion of BAO data in the analysis causes H_0 in the Λ_s CDM + $N_{\text{eff}} + \sum m_{\nu}$ to approach values similar to those in Λ CDM + $N_{\text{eff}} + \sum m_{\nu}$, as the effect of the mirror AdS-dS transition is weakened. This is particularly due to the low-redshift BAO data points (see, e.g., Refs. [60, 63] for a discussion of low-redshift BAO in the context of Λ_s CDM), which provide only lower bounds on z_{\dagger} —specifically $z_{\dagger} > 1.69$ for Planck+BAO and $z_{\dagger} > 1.65$ for Planck+BAO+PP&SH0ES at 95% CL—leaving z_{\dagger} unbounded from above and thereby allowing the Λ CDM limit of the Λ_s framework. Notably, for the base model, these bounds are $z_{\dagger} > 2.11$ at 95% CL and $z_{\dagger} = 2.31_{-0.36}^{+0.15}$ at 68% CL. Only a moderate improvement in H_0 tension is achieved in the case of Planck+BAO+PP&SH0ES with $N_{\text{eff}} = 3.44 \pm 0.15$ and $H_0 = 71.09_{-0.70}^{+0.81}$ km s⁻¹ Mpc⁻¹. However, this improvement arises mainly from the relatively substantial increase in N_{eff} , which modifies the pre-recombination universe by reducing r_d (and r_*) along with θ_s compared to the base models, rather than the mirror AdS-dS transition. For the base Λ_s CDM model, the combined Planck+BAO+PP&SH0ES dataset yields $H_0 = 69.82 \pm 0.49$ km s⁻¹ Mpc⁻¹ [63]. In contrast, with the extended Λ_s CDM model using Planck+BAO, we find $H_0 = 67.20 \pm 1.20$ km s⁻¹ Mpc⁻¹, which is lower than the base model’s value of $H_0 = 68.92 \pm 0.49$ km s⁻¹ Mpc⁻¹ [63] and even falls below the mean value for the base Λ CDM model, despite allowing lower values of z_{\dagger} ($z_{\dagger} > 1.69$ at 95% CL). This reduction can be attributed to the mean value of $N_{\text{eff}} = 2.87 \pm 0.19$ (68% CL), which is slightly below the standard value of 3.044. We stress here the fact that the BAO (3D BAO) data, which implicitly assume Planck- Λ CDM as fiducial cosmology in computing the distance to the spherical shell (see also Footnote 2), push Λ_s CDM + $N_{\text{eff}} + \sum m_{\nu}$ towards Λ CDM + $N_{\text{eff}} + \sum m_{\nu}$, posing an impediment to the efficient operation of the mirror AdS-dS transition mechanism, hence to the resolution of the tensions. As a reference to better contextu-

alize the findings presented here, it is worth commenting on the canonical cosmological models extending beyond Λ CDM, such as w CDM (a one-parameter extension of the standard Λ CDM model, where DE is characterized by a constant EoS parameter) and w_0w_a CDM (a two-parameter extension employing the CPL parametrization for DE), which are among the most commonly explored frameworks for examining deviations in neutrino properties from their SM predictions and their impacts on cosmological dynamics, viz., the w CDM + $N_{\text{eff}} / \sum m_{\nu}$ and w_0w_a CDM + $N_{\text{eff}} / \sum m_{\nu}$ models. In the case of w CDM extended by N_{eff} and $\sum m_{\nu}$, the DE EoS parameter typically returns values consistent with a cosmological constant (i.e., minus unity) when analyzed with Planck+BAO and Planck+BAO+SNe, yielding $H_0 \sim 68$ km s⁻¹ Mpc⁻¹ and $S_8 \sim 0.82$ —values that closely mirror those obtained in the base Λ CDM model—thereby failing to address either the H_0 or S_8 tensions and showing no significant deviation from the standard N_{eff} and $\sum m_{\nu}$ values. Worse still, while the w_0w_a CDM + $N_{\text{eff}} / \sum m_{\nu}$ models exhibit similar trends for Planck+BAO+SNe, their confrontation with the Planck+BAO dataset exacerbates the H_0 tension, driving the value down to $H_0 \sim 65$ km s⁻¹ Mpc⁻¹, despite the increased number of model parameters and the consequently enlarged uncertainties. See, for instance, Refs. [155, 223], as well as Refs. [146, 153, 156, 224], along with the references therein, for further discussions on the constraints on neutrino properties and their implications for cosmological dynamics within canonical extensions of the standard Λ CDM model. On the other hand, the combined Planck+BAOtr and Planck+BAOtr+PP&SH0ES datasets, incorporating the weakly model-dependent BAOtr data, yield $H_0 = 73.10 \pm 1.40$ km s⁻¹ Mpc⁻¹ and $H_0 = 73.08 \pm 0.76$ km s⁻¹ Mpc⁻¹ for the Λ_s CDM + $N_{\text{eff}} + \sum m_{\nu}$ model, respectively, in excellent agreement with the SH0ES measurement of $H_0 = 73.04 \pm 1.04$ km s⁻¹ Mpc⁻¹ [25]. However, despite the evident improvement in H_0 for Λ CDM + $N_{\text{eff}} + \sum m_{\nu}$ as well—specifically, $H_0 = 70.10 \pm 1.30$ km s⁻¹ Mpc⁻¹ and $H_0 = 72.23 \pm 0.74$ km s⁻¹ Mpc⁻¹, respectively—this enhancement comes at the cost of a significant divergence from the SM of particle physics, altering the pre-recombination universe by modifying the sound horizon r_d and the angular scale θ_s relative to the base models. For reference, using the same dataset, the base Λ CDM model yields values of $H_0 = 68.84 \pm 0.48$ km s⁻¹ Mpc⁻¹ and $H_0 = 69.57 \pm 0.42$ km s⁻¹ Mpc⁻¹, correspondingly. Particularly, in the case of Planck+BAOtr+PP&SH0ES, the predicted $N_{\text{eff}} = 3.50 \pm 0.13$ from the Λ CDM + $N_{\text{eff}} + \sum m_{\nu}$ model results in a 3.5σ tension with the SM value of $N_{\text{eff}} = 3.044$, accompanied by a corresponding reduction in r_d that also deviates at a 3.5σ level from the base Λ CDM constraint, when using the same dataset [61]. In contrast, in the Λ_s CDM + $N_{\text{eff}} + \sum m_{\nu}$ model, we obtain $N_{\text{eff}} = 3.11_{-0.15}^{+0.13}$, which is fully consistent with SM value of $N_{\text{eff}} = 3.044$ within 68% CL interval, aligning with the observation that there is no significant reduction in r_d compared to the base Λ_s CDM constraint when using

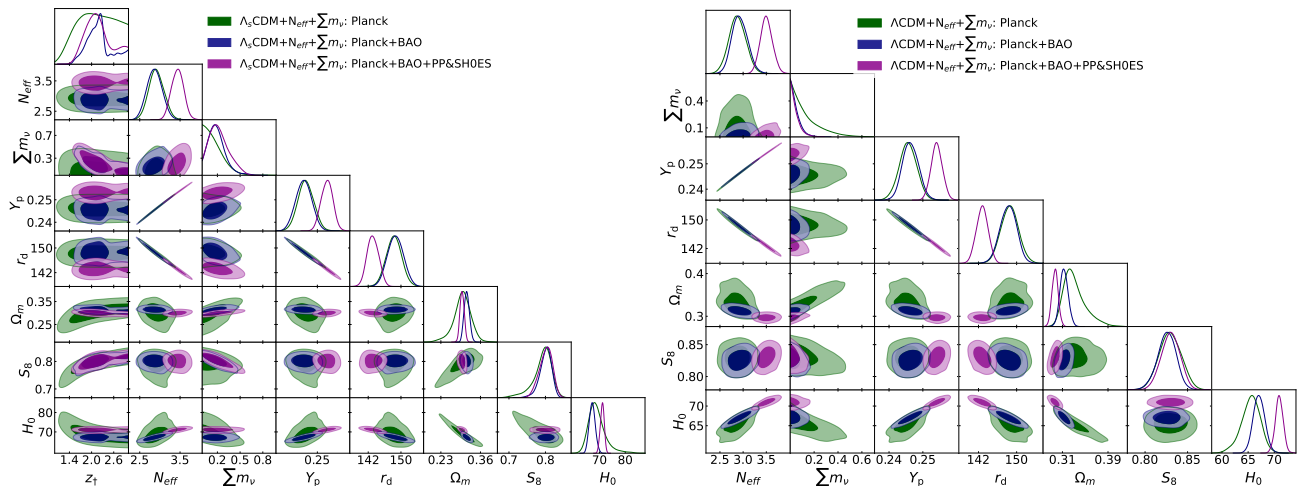


FIG. 1. Marginalized posterior distributions and contours (68% and 95% CL) of $\Lambda_s\text{CDM}+N_{\text{eff}}+\sum m_\nu$ (Left) and $\Lambda\text{CDM}+N_{\text{eff}}+\sum m_\nu$ (Right) model parameters for the Planck (green), Planck+BAO (blue), and Planck+BAO+PP&SH0ES (magenta) datasets.

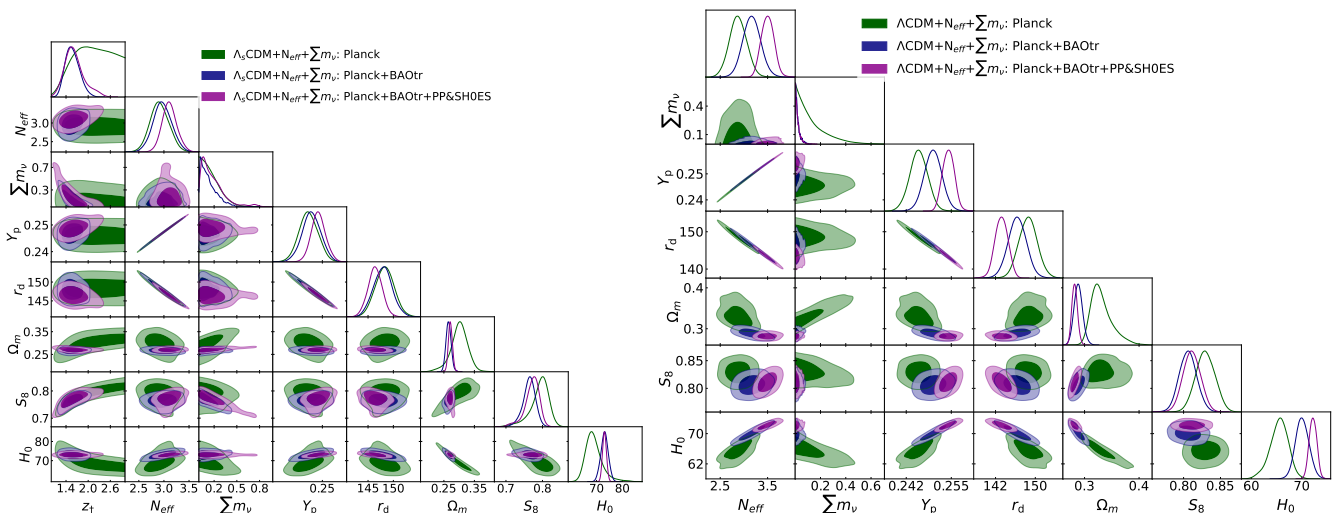


FIG. 2. Marginalized posterior distributions and contours (68% and 95% CL) of $\Lambda_s\text{CDM}+N_{\text{eff}}+\sum m_\nu$ (Left) and $\Lambda\text{CDM}+N_{\text{eff}}+\sum m_\nu$ (Right) model parameters for the Planck (green), Planck+BAOtr (blue), and Planck+BAOtr+PP&SH0ES (magenta) datasets.

the same dataset [61]. Before concluding our discussion with a focus on the implications of our results for the H_0 tension, it is worth noting that two-parameter extensions incorporating N_{eff} and $\sum m_\nu$ have also been explored in the literature for various models proposed to address the H_0 tension, while also considering the S_8 tension. Similar to our investigation of the $\Lambda_s\text{CDM}+N_{\text{eff}}+\sum m_\nu$ extension of the abrupt $\Lambda_s\text{CDM}$ model, examples include the PEDE + $N_{\text{eff}}+\sum m_\nu$, IDE + $N_{\text{eff}}+\sum m_\nu$, and VM + $N_{\text{eff}}+\sum m_\nu$ models [144, 225–227], which extend the frameworks of PEDE (Phenomenologically Emergent Dark Energy), IDE (Interacting Dark Energy), and VM (Vacuum Metamorphosis), respectively.

The H_0 tension also shows up in the supernova absolute magnitude M_B , determined through the Cepheid calibra-

tion, as a $\sim 3.4\sigma$ discrepancy with the results obtained by the inverse distance ladder method utilizing the sound horizon r_d as calibrator [191], via the distance modulus $\mu(z_i) = m_{B,i} - M_{B,i}$, where $\mu(z_i) = 5 \log_{10} \left(\frac{1+z_i}{10 \text{ pc}} \int_0^{z_i} \frac{cdz}{H(z)} \right)$ in the spatially flat Robertson-Walker spacetime, and $m_{B,i}$ is the SNIa apparent magnitude measured at the redshift z_i . In the case of Planck+BAO+PP&SH0ES, both extended models yield similar values of $M_B \approx -19.33$ mag, which are in 2σ tension with the SH0ES calibrated value of $M_B = -19.244 \pm 0.037$ mag [218]. This 2σ tension is reduced to 0.9σ when the BAOtr is used instead of BAO for the $\Lambda_s\text{CDM}+N_{\text{eff}}+\sum m_\nu$ model. Specifically, using the combined Planck+BAOtr+PP&SH0ES dataset results in $M_B = -19.281 \pm 0.021$ mag for the $\Lambda_s\text{CDM}+N_{\text{eff}}+\sum m_\nu$

TABLE II. The concordance/discordance between the $\Lambda\text{CDM}+N_{\text{eff}}+\sum m_\nu / \Lambda_s\text{CDM}+N_{\text{eff}}+\sum m_\nu$ models and the estimations derived from theoretical predictions or direct observations: $H_0 = 73.04 \pm 1.04 \text{ km s}^{-1} \text{ Mpc}^{-1}$ of the SH0ES measurement [217]; $M_B = -19.244 \pm 0.037 \text{ mag}$ (SH0ES) [218]; $N_{\text{eff}}^{\text{SM}} = 3.044$, the effective number of neutrino species calculated in the framework of the standard model of particle physics [166–168]; primordial helium abundances $Y_{\text{p}}^{\text{Aver et al.}} = 0.2453 \pm 0.0034$ and $Y_{\text{p}}^{\text{Fields et al.}} = 0.2469 \pm 0.0002$ [219, 220]; $10^2 \omega_{\text{b}}^{\text{LUNA}} = 2.233 \pm 0.036$ (empirical approach, based primarily on experimentally measured cross sections for $d(p, \gamma)^3\text{He}$ reaction) [221] and $10^2 \omega_{\text{b}}^{\text{PCUV21}} = 2.195 \pm 0.022$ (theoretical approach, incorporating nuclear theory for $d(p, \gamma)^3\text{He}$ reaction) [222]. $S_8 = 0.746_{-0.021}^{+0.026}$ of $\Lambda_s\text{CDM:KiDS-1000}$ and $S_8 = 0.749_{-0.020}^{+0.027}$ of $\Lambda\text{CDM:KiDS-1000}$ [61].

Dataset	Planck	Planck+BAO	Planck+BAOtr	Planck+BAO +PP&SH0ES	Planck+BAOtr +PP&SH0ES
Model	$\Lambda_s\text{CDM}+N_{\text{eff}}+\sum m_\nu$				
	$\Lambda\text{CDM}+N_{\text{eff}}+\sum m_\nu$				
H_0	1.3 σ	3.7 σ	0.0 σ	1.5 σ	0.0 σ
	3.6 σ	3.9 σ	1.8 σ	1.6 σ	0.6 σ
M_B	-	-	-	2.0 σ	0.9 σ
	-	-	-	2.1 σ	2.0 σ
S_8	1.4 σ	1.9 σ	0.6 σ	1.9 σ	0.8 σ
	3.0 σ	2.9 σ	2.2 σ	3.2 σ	2.4 σ
N_{eff}	0.7 σ	0.9 σ	0.4 σ	2.6 σ	0.5 σ
	0.9 σ	0.7 σ	0.7 σ	3.5 σ	3.5 σ
Y_{p} (Aver et al.)	0.2 σ	0.0 σ	0.4 σ	2.0 σ	0.9 σ
	0.1 σ	0.3 σ	1.0 σ	2.3 σ	2.3 σ
Y_{p} (Fields et al.)	0.3 σ	0.6 σ	0.0 σ	3.1 σ	1.0 σ
	0.5 σ	0.2 σ	1.1 σ	4.2 σ	4.3 σ
ω_{b} (PCUV21)	1.0 σ	0.8 σ	1.5 σ	2.5 σ	1.8 σ
	0.7 σ	1.4 σ	2.6 σ	3.3 σ	4.0 σ
ω_{b} (LUNA)	0.1 σ	0.4 σ	0.1 σ	0.8 σ	0.3 σ
	0.4 σ	0.0 σ	0.9 σ	1.3 σ	1.7 σ

model, whereas the tension remains at the 2σ level in the $\Lambda\text{CDM} + N_{\text{eff}} + \sum m_\nu$ model.

Furthermore, when N_{eff} and $\sum m_\nu$ are relaxed within the context of ΛCDM , analyses from Planck, Planck+BAO, and Planck+BAO+PP&SH0ES yield upper bounds of $\sum m_\nu < 0.40 \text{ eV}$, $\sum m_\nu < 0.13 \text{ eV}$, and $\sum m_\nu < 0.13 \text{ eV}$, respectively. Notably, the latter two values, $\sum m_\nu < 0.13 \text{ eV}$, are exceedingly stringent, bordering on the threshold that would rule out IH, where $\sum m_\nu > 0.1 \text{ eV}$. Moreover, the combined datasets Planck+BAOtr and Planck+BAOtr+PP&SH0ES favor an even lower sum of neutrino masses, with $\sum m_\nu < 0.06 \text{ eV}$. These upper limits are in stark contrast to the lower bounds established by flavor oscillation experiments, implying an additional complication alongside the need for new physics suggested by $\Delta N_{\text{eff}} > 0$. On the other hand, using the $\Lambda_s\text{CDM} + N_{\text{eff}} + \sum m_\nu$ model, the upper bounds range from $\sum m_\nu < 0.35 \text{ eV}$ to $\sum m_\nu < 0.49 \text{ eV}$. Both bounds are completely concordant with experimental results. Similarly, in the $w_0 w_a \text{CDM} + \sum m_\nu$ model, certain dataset combinations, including CMB, BAO, and SNIa data, supplemented by the τ prior, impose comparable upper bounds on $\sum m_\nu$, as demonstrated in [153]. Notably, when the dark energy EoS is restricted to the quintessence region, i.e., $w(z) \geq -1$, these bounds tighten slightly compared to ΛCDM , despite the increased number of free parameters. This tightening trend is further corroborated by more recent analyses incorporating DESI BAO data,

as reported in Ref. [224].

Furthermore, as shown in Table II, the $\Lambda\text{CDM} + N_{\text{eff}} + \sum m_\nu$ model exhibits a $2.5 - 3\sigma$ tension with the low redshift measurements of S_8 , e.g., $S_8 = 0.759_{-0.021}^{+0.024}$ [31] (also reported as $S_8 = 0.749_{-0.020}^{+0.027}$ in Refs. [61, 63]) from KiDS-1000 data, obtained within the standard ΛCDM framework. This indicates that there is almost no reduction in the significance of the S_8 tension, suggesting that it persists in the extended ΛCDM model without exception. On the other hand, the $\Lambda_s\text{CDM} + N_{\text{eff}} + \sum m_\nu$ model performs significantly better, exhibiting no S_8 tension at all when combined Planck, Planck+BAOtr, and Planck+BAOtr+PP&SH0ES datasets are used. These datasets predict S_8 values in excellent alignment with $S_8 = 0.746_{-0.021}^{+0.026}$ [61, 63] derived from KiDS-1000 alone for the base (abrupt) $\Lambda_s\text{CDM}$ model. Moreover, it reduces the tension to 1.9σ even for the Planck+BAO and Planck+BAO+PP&SH0ES datasets. Interestingly, despite the matter density parameter Ω_{m} of $\Lambda_s\text{CDM} + N_{\text{eff}} + \sum m_\nu$ trending towards higher values—similar to those in the $\Lambda\text{CDM} + N_{\text{eff}} + \sum m_\nu$ model—due to the influence of low-redshift BAO data points in the Planck+BAO and Planck+BAO+PP&SH0ES datasets, it still manages to yield reasonably lower S_8 values. This outcome arises because the effectiveness of the two-parameter extension of the $\Lambda_s\text{CDM}$ model in mitigating the S_8 tension stems from the interplay between the total neutrino mass $\sum m_\nu$ and the late-time mirror AdS-to-

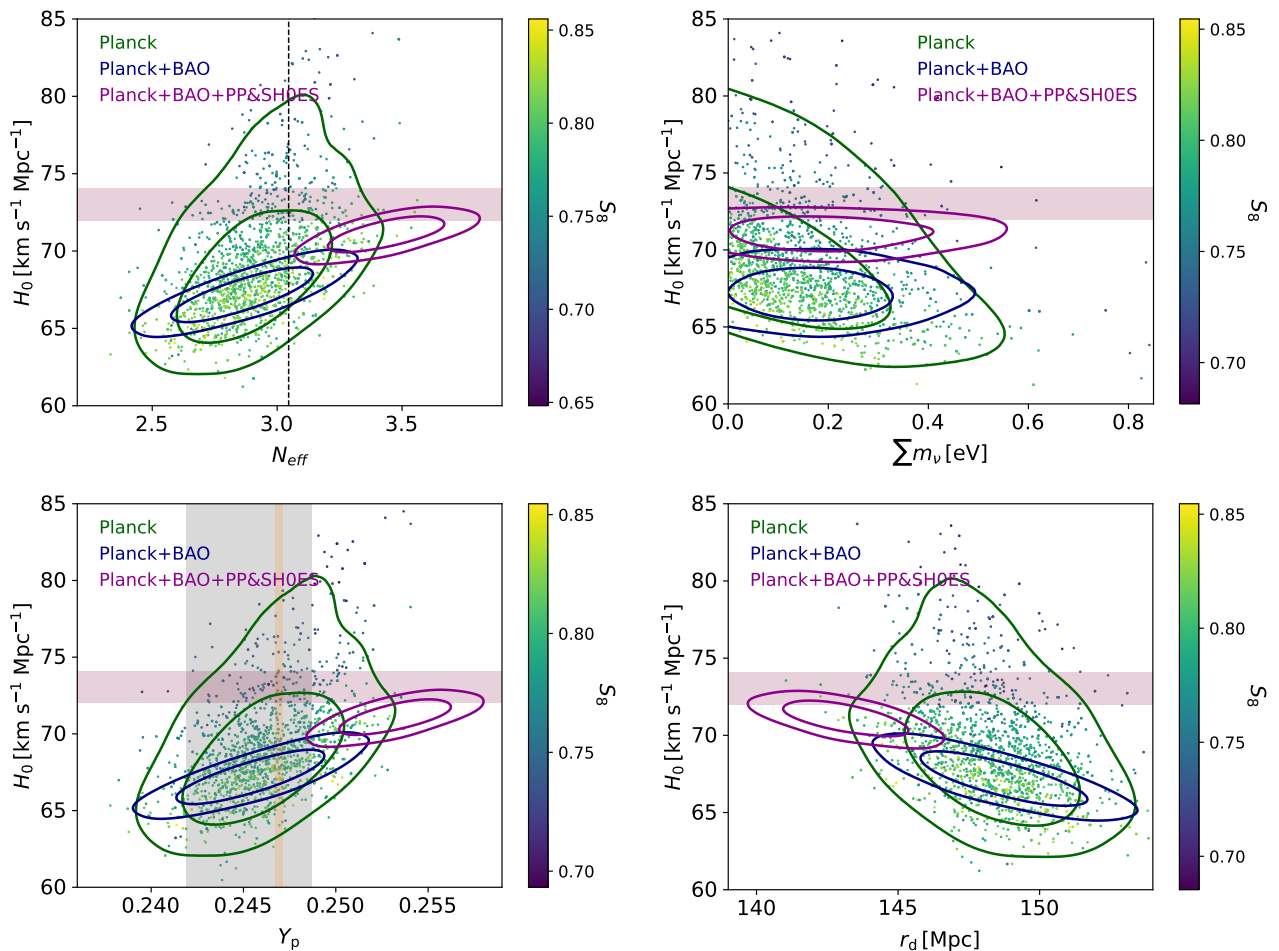


FIG. 3. Two-dimensional marginalized posterior distributions (68% and 95% CL) in the $H_0 - N_{\text{eff}}$ (upper left), $H_0 - \sum m_\nu$ (upper right), $H_0 - Y_p$ (lower left) and $H_0 - r_d$ (lower right) planes, color-coded (Planck Only data) by S_8 for the $\Lambda_s\text{CDM} + N_{\text{eff}} + \sum m_\nu$ model, considering different combinations of datasets. The horizontal magenta band represents the SH0ES measurement $H_0 = 73.04 \pm 1.04 \text{ km s}^{-1} \text{ Mpc}^{-1}$ (68% CL) [25]. Additionally, the vertical grey and yellow bands for $Y_p^{\text{Aver et al.}} = 0.2453 \pm 0.0034$ [219] and $Y_p^{\text{Fields et al.}} = 0.2469 \pm 0.0002$ [220], respectively.

dS transition mechanism. As shown in Figs. 1 and 2, $\sum m_\nu$ is anti-correlated with S_8 in both models, especially when analyzed with the Planck+BAOtr/BAO and Planck+BAOtr/BAO+PP&SH0ES datasets. This implies that larger $\sum m_\nu$ values suppress σ_8 more effectively. On the other hand, since $\sum m_\nu$ is degenerate with H_0 , as seen in Fig. 2, achieving relatively higher H_0 values within the $\Lambda\text{CDM} + N_{\text{eff}} + \sum m_\nu$ model necessitates neutrinos being less massive. This also explains the rather stringent constraints, $\sum m_\nu < 0.06$ (< 0.13) eV, $\sum m_\nu < 0.06$ (< 0.13) eV imposed by the Planck+BAOtr(BAO) and Planck+BAOtr(BAO)+PP&SH0ES datasets, respectively. Consequently, a sufficiently large reduction in S_8 through the suppression of σ_8 , necessary to match $S_8 = 0.759^{+0.024}_{-0.021}$ from ΛCDM -KiDS [31], cannot be achieved. Furthermore, the obtained Ω_m values, $\Omega_m \gtrsim 0.29$, are not low enough to aid in resolving the S_8 tension. These findings indicate that $\Lambda\text{CDM} + N_{\text{eff}} + \sum m_\nu$ cannot simultaneously address both H_0 and S_8 tensions with-

out a trade-off. However, note that the upper bounds $\sum m_\nu \lesssim 0.50$ eV provided by the Planck+BAOtr/BAO and Planck+BAOtr/BAO+PP&SH0ES datasets for the $\Lambda_s\text{CDM} + N_{\text{eff}} + \sum m_\nu$ model are much less stringent than those obtained in the $\Lambda\text{CDM} + N_{\text{eff}} + \sum m_\nu$ model. Consequently, neutrinos in the extended $\Lambda_s\text{CDM}$ are allowed to be 3 to 8 times more massive, thanks to the late-time mirror AdS-to-dS transition mechanism. This indirectly results in smaller σ_8 values by permitting larger $\sum m_\nu$.⁶ To some extent, this enables the model to circumvent the BAO data's tendency to exacerbate the S_8 tension via elevated Ω_m values. Nevertheless, for Planck+BAOtr and Planck+BAOtr+PP&SH0ES datasets, the transition

⁶ For a similar motivation, see, for example, Ref. [49], which explores the suppressive effect of massive neutrinos on σ_8 as a means to mitigate the typical exacerbation of the S_8 tension by early dark energy (EDE) models.

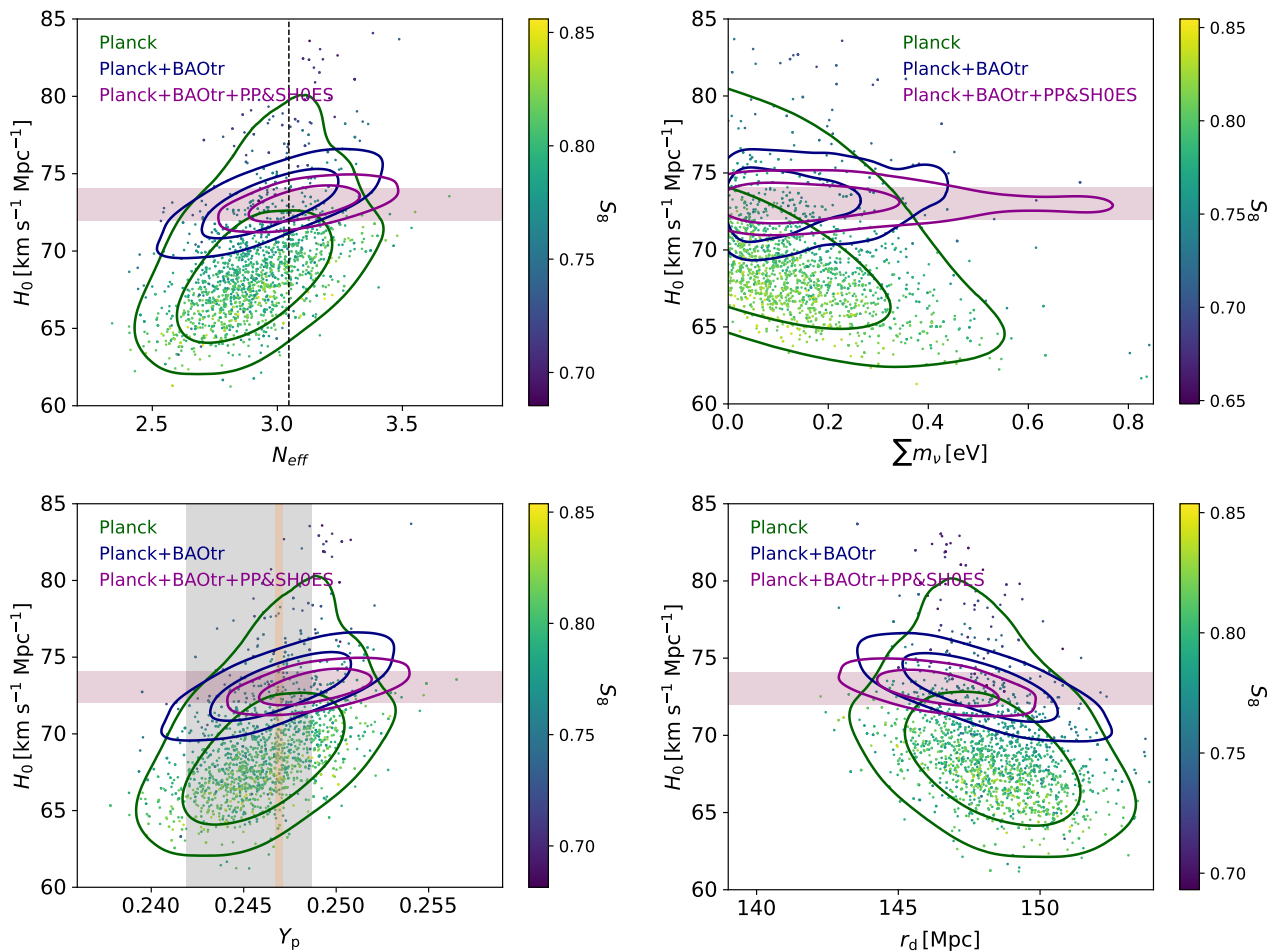


FIG. 4. Two-dimensional marginalized posterior distributions (68% and 95% CL) in the $H_0 - N_{\text{eff}}$ (upper left), $H_0 - \sum m_\nu$ (upper right), $H_0 - Y_p$ (lower left) and $H_0 - r_d$ (lower right) planes, color-coded (Planck Only data) by S_8 for the $\Lambda_s\text{CDM} + N_{\text{eff}} + \sum m_\nu$ model, considering different combinations of datasets. The horizontal magenta band represents the SH0ES measurement $H_0 = 73.04 \pm 1.04 \text{ km s}^{-1} \text{ Mpc}^{-1}$ (68% CL) [25]. Additionally, the vertical grey and yellow bands for $Y_p^{\text{Aver et al.}} = 0.2453 \pm 0.0034$ [219] and $Y_p^{\text{Fields et al.}} = 0.2469 \pm 0.0002$ [220], respectively.

mechanism becomes more prominent at lower redshifts, viz., $z_\dagger \sim 1.6$, resulting in an enhanced H_0 , and, consequently, a lower Ω_m compared to the extended ΛCDM model. Given that $S_8 = \sigma_8 \sqrt{\Omega_m/0.3}$, the allowance for more massive neutrinos works synergistically with z_\dagger to reduce S_8 to even more compatible values, such as $S_8 = 0.763^{+0.019}_{-0.014}$ and $S_8 = 0.771^{+0.022}_{-0.014}$, which align perfectly with $S_8 = 0.746^{+0.026}_{-0.021}$ from the base $\Lambda_s\text{CDM}$ -KiDS 1000 analysis [61]. Notably, there remains significant tension between the Planck data and the PP&SH0ES data within the ΛCDM model.

In Table I, we observe that when N_{eff} is allowed to vary (i.e., in the extended models), the PP&SH0ES dataset favors $\Delta N_{\text{eff}} > 0$, resulting in higher H_0 values compared to the base counterparts of both extended models, where N_{eff} is fixed at the standard value of $N_{\text{eff}} = 3.044$ (see Refs. [59–61]). An immediate consequence is that the freeze-out temperature T_f , and thus the corresponding baryon density ω_b , increases due to $\Delta N_{\text{eff}} > 0$. This

manifests as a positive correlation between N_{eff} and ω_b [or a negative correlation between r_* (and r_d) and ω_b], leading to predicted primordial helium-4 abundances that exceed expected levels, as discussed in Section II C. These elevated levels are particularly discrepant with astrophysical measurements in the context of the extended ΛCDM model. In the $\Lambda\text{CDM} + N_{\text{eff}} + \sum m_\nu$ model, the Planck+BAOtr+PP&SH0ES dataset favors a primordial helium-4 abundance, $Y_p = 0.2542 \pm 0.0017$, in 2.3σ and 4.3σ tensions with $Y_p^{\text{Aver et al.}} = 0.2453 \pm 0.0034$ [219] and $Y_p^{\text{Fields et al.}} = 0.2469 \pm 0.0002$ [220], respectively. Notably, this prediction of Y_p is also in 3.6σ tension with its base ΛCDM prediction from the same dataset, which yields $Y_p = 0.248010 \pm 0.000056$ [61], as expected, paralleling our previous discussion on N_{eff} within the ΛCDM framework, comparing the extended and base versions for this dataset. A similar situation arises for the Planck+BAO+PP&SH0ES dataset, which estimates $Y_p = 0.2541 \pm 0.0017$, resulting in tensions of 2.3σ and 4.2σ with

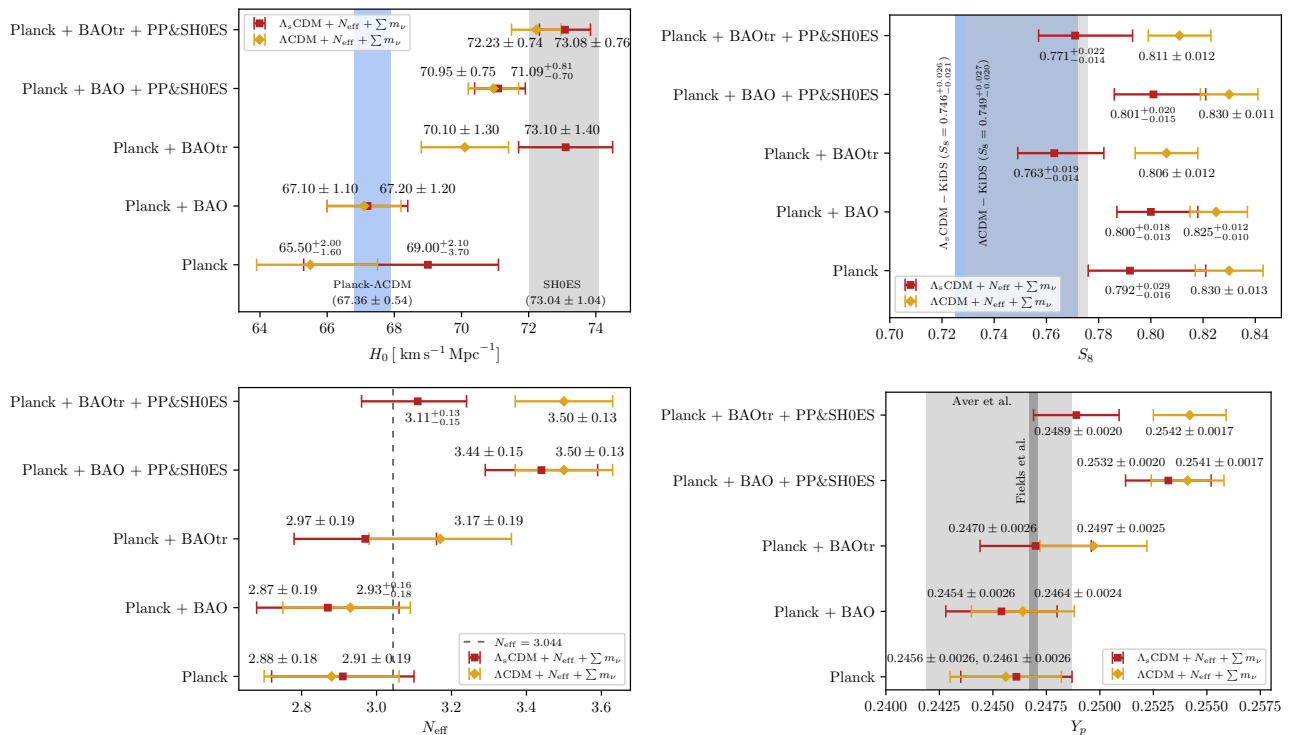


FIG. 5. In these whisker plots, we present mean values with 68% CL obtained for $\Lambda_s\text{CDM} + N_{\text{eff}} + \sum m_\nu$ and $\Lambda\text{CDM} + N_{\text{eff}} + \sum m_\nu$ and shaded bands represent various cosmological observations and predictions. In the upper left panel we compare the Hubble constants H_0 of both models to the SH0ES measurement $H_0 = 73.04 \pm 1.04 \text{ km s}^{-1} \text{ Mpc}^{-1}$ [25] and the Planck- ΛCDM value $H_0 = 67.36 \pm 0.54 \text{ km s}^{-1} \text{ Mpc}^{-1}$ [3]. Notice that H_0 values predicted by $\Lambda_s\text{CDM} + N_{\text{eff}} + \sum m_\nu$ lie well within the region of local H_0 measurements when a weakly model-dependent dataset BAOtr is included in the analysis. In the upper right, we confront S_8 values with those found by KiDS in the context of both ΛCDM and $\Lambda_s\text{CDM}$, $S_8 = 0.746^{+0.026}_{-0.020}$ of $\Lambda_s\text{CDM-KiDS}$ and $S_8 = 0.749^{+0.027}_{-0.020}$ of $\Lambda\text{CDM-KiDS}$ [61]. Similarly $\Lambda_s\text{CDM} + N_{\text{eff}} + \sum m_\nu$ fully resolves the S_8 tension for datasets with BAOtr, and alleviates it at the worst cases. The lower left panel displays the deviation of N_{eff} from the standard value $N_{\text{eff}} = 3.044$ predicted in particle physics [166–168], with which $\Lambda_s\text{CDM} + N_{\text{eff}} + \sum m_\nu$ is compatible, except in the case of the BAO dataset. Lastly at the lower right, we confront the predicted abundance of primeval helium-4 with the results found in astrophysical observations. We see a very similar pattern to that of N_{eff} here as N_{eff} and Y_p are strongly correlated. Overall $\Lambda_s\text{CDM} + N_{\text{eff}} + \sum m_\nu$ agrees much better with the observed values $Y_p^{\text{Aver et al.}} = 0.2453 \pm 0.0034$ and $Y_p^{\text{Fields et al.}} = 0.2469 \pm 0.0002$ [219, 220].

these measurements. However, for the $\Lambda_s\text{CDM} + N_{\text{eff}} + \sum m_\nu$ model using the same Planck+BAOtr+PP&SH0ES dataset, we find $Y_p = 0.2489 \pm 0.0020$, which aligns within 1.0σ with both sets of measurements, indicating no tension at all. Moreover, this prediction is in excellent agreement with the base $\Lambda_s\text{CDM}$ prediction of $Y_p = 0.247877 \pm 0.000061$ from the same dataset, showing only a 0.5σ deviation. This result also aligns with our earlier discussion on N_{eff} within the $\Lambda_s\text{CDM}$ framework, comparing the extended and base versions for this dataset. As with H_0 , the incorporation of BAO into the analysis hinders the reconciliation of Y_p predicted by $\Lambda_s\text{CDM} + N_{\text{eff}} + \sum m_\nu$ with direct measurements. Nonetheless, the statistical significance of the tensions from the value $Y_p = 0.2532 \pm 0.0020$ are at 2σ and 3.1σ , both of which are still more favorable than those found for $\Lambda\text{CDM} + N_{\text{eff}} + \sum m_\nu$. This suggests that resolving the H_0 and S_8 tensions without introducing new significant discrepancies with astrophysical observations of the pri-

mordial helium mass fraction, Y_p , cannot be achieved by simply allowing N_{eff} and $\sum m_\nu$ as two additional free parameters in the standard ΛCDM model. However, within the $\Lambda_s\text{CDM} + N_{\text{eff}} + \sum m_\nu$ framework, it is possible to address both H_0 and S_8 discrepancies without creating significant tensions in parameters like Y_p and N_{eff} . It is crucial to note that the resolution of these tensions in the extended $\Lambda_s\text{CDM}$ model is not due to a broadening of error bars but primarily to an overall shift in the central values of the relevant parameters in the correct direction, as illustrated in Fig. 5.

Last but not least, to assess the goodness and robustness of the statistical fit to the observational data, we provide a quantitative comparison between the $\Lambda_s\text{CDM} + N_{\text{eff}} + \sum m_\nu$ and $\Lambda\text{CDM} + N_{\text{eff}} + \sum m_\nu$ models in terms of relative log-Bayesian evidence, $\ln \mathcal{B}_{ij}$, according to the updated Jeffreys’ scale [215, 216]. The analysis yields inconclusive Bayesian evidence ($\ln \mathcal{B}_{ij} = -0.63$) between models for the CMB-alone case. In contrast,

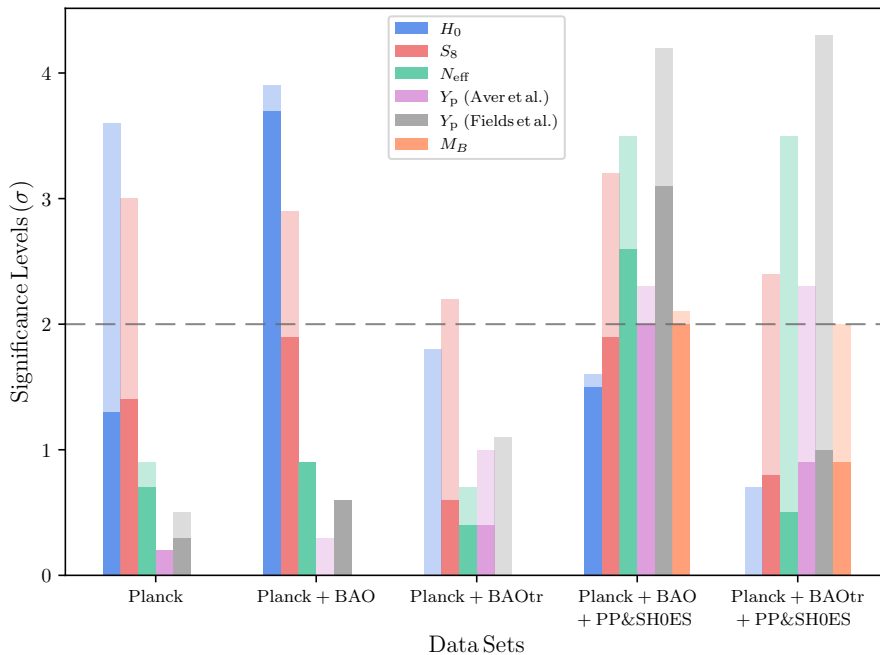


FIG. 6. We here illustrate the statistical significance of various tensions encompassing H_0 , M_B , S_8 , N_{eff} and Y_p in the bar chart where the bars in dark colors represent the relevant tensions in $\Lambda_s\text{CDM} + N_{\text{eff}} + \sum m_\nu$ and the bars in faded colors correspond to their counterparts in $\Lambda\text{CDM} + N_{\text{eff}} + \sum m_\nu$. Notice that the $\Lambda_s\text{CDM}$ extension outclasses the ΛCDM one across the entire datasets in both addressing the current discrepancies and retaining the consistencies already established in the standard model. Besides, it does not suffer from any tension other than BAO-induced H_0 tension of 3.7σ and N_{eff} tension of mild 2.6σ (and the associated 3.1σ Y_p), the reason of which we have emphasized for a couple of times in Section IV.

we find weak statistical evidence in favor of $\Lambda_s\text{CDM} + N_{\text{eff}} + \sum m_\nu$ when incorporating BAO datasets, with $\ln \mathcal{B}_{ij} = -1.98$ for Planck+BAO and $\ln \mathcal{B}_{ij} = -1.24$ for Planck+BAO+PP&SH0ES. Remarkably, this preference is significantly enhanced to a very strong level by substituting BAOtr for BAO, yielding evidence values of $\ln \mathcal{B}_{ij} = -11.73$ and $\ln \mathcal{B}_{ij} = -11.05$ for Planck+BAOtr and Planck+BAOtr+PP&SH0ES, respectively.

Consequently, we infer that the $N_{\text{eff}} + \sum m_\nu$ extension of the $\Lambda_s\text{CDM}$ model outperforms the ΛCDM extension in fitting the data, addressing the H_0 and S_8 tensions, and maintaining coherence with well-established theoretical predictions and observations across all datasets, as demonstrated in Figs. 5 and 6. Additionally, we provide a bar chart in Fig. 6 that summarizes and visually illustrates the statistical significance of various concordances and discordances (tensions) across key cosmological and astrophysical parameters— H_0 , M_B , S_8 , N_{eff} , and Y_p . This comprehensive visualization reinforces our conviction that to gain a deeper understanding of the cosmos through independent observations, incorporating new physics at later times is an indispensable component of our exploration, if not the sole resolutions to the tensions.

A. Consistency with the AAL- $\Lambda_s\text{CDM}$ model

It has recently been reported in Ref. [66–68] that the mirror AdS to dS transition at low energies (in the late universe at $z \sim 2$), which characterizes the $\Lambda_s\text{CDM}$ model, can be realized through the Casimir forces inhabiting the bulk. This fundamental physical mechanism, proposed to substantiate the $\Lambda_s\text{CDM}$ model, suggests that the effective number of relativistic neutrino species, N_{eff} , is altered by the fields that characterize the deep infrared region of the dark sector, resulting in a deviation $\Delta N_{\text{eff}} \approx 0.25$ from the standard model value of particles physics. We refer to this particular realization of the $\Lambda_s\text{CDM}$ model as AAL- $\Lambda_s\text{CDM}$. As we previously discussed, an increase in N_{eff} modifies the standard BBN by increasing the expansion rate during the BBN epoch, which leads to greater abundances of primordial Helium-4. The impact of small modifications in the expansion rate of the universe during the BBN epoch on the helium-4 mass fraction, Y_p , can approximately be quantified using an analytical formula provided by Ref. [228]:

$$Y_p = 0.2381 \pm 0.0006 + 0.0016[\eta_{10} + 100(S - 1)], \quad (11)$$

where η_{10} represents the scaled baryon-to-photon ratio ($\eta_{10} = 273.9\omega_b$). The parameter S , quantifying the deviation of the expansion rate during the BBN epoch, H'_{BBN} , from the expansion rate in the standard BBN model,

H_{SBBN} , due to additional relativistic species, is given by:

$$S = \frac{H'_{\text{BBN}}}{H_{\text{SBBN}}} = \sqrt{1 + \frac{7}{43}\Delta N_{\text{eff}}}. \quad (12)$$

We then assess the implications of the prediction $\Delta N_{\text{eff}} \approx 0.25$ within the framework of $\Lambda_s\text{CDM} + N_{\text{eff}} + \sum m_\nu$ and calculate $Y_{\text{p}}^{\text{AAL}} = 0.2512 \pm 0.0006$, which we compare with the mass fractions obtained from the observational analysis detailed in Table III. For the dataset combinations Planck+BAOtr, Planck+BAO+PP&SH0ES, and Planck+BAOtr+PP&SH0ES, the AAL- $\Lambda_s\text{CDM}$ predicted abundance for $\Delta N_{\text{eff}} \approx 0.25$ is consistent with the abundances found in $\Lambda_s\text{CDM} + N_{\text{eff}} + \sum m_\nu$ at less than 2σ . As expected, the same holds for the effective number of neutrino species, $N_{\text{eff}} = 3.294$, since Y_{p} and N_{eff} are strongly and positively correlated. In the last two rows of the table, we observe that a 3.3σ tension in Y_{p} emerges due to the relaxation of N_{eff} when $\Lambda\text{CDM} + N_{\text{eff}} + \sum m_\nu$ is analyzed using the Planck+BAO+PP&SH0ES and Planck+BAOtr+PP&SH0ES datasets. In contrast, for $\Lambda_s\text{CDM} + N_{\text{eff}} + \sum m_\nu$, the tension is a mild 2.5σ and non-existent in the case of Planck+BAO+PP&SH0ES and Planck+BAOtr+PP&SH0ES, respectively. Thus, while the $\Lambda_s\text{CDM} + N_{\text{eff}} + \sum m_\nu$ model, when confronted with observational data, yields N_{eff} and Y_{p} values that are much more compatible with standard BBN than those of the $\Lambda\text{CDM} + N_{\text{eff}} + \sum m_\nu$ model, the constraints on N_{eff} and Y_{p} are still compatible with their predicted values in the AAL- $\Lambda_s\text{CDM}$ model within $\sim 2\sigma$. This suggests that the AAL- $\Lambda_s\text{CDM}$ could achieve similar success in fitting the data as the $\Lambda_s\text{CDM}$ model. Nevertheless, to definitely confirm our conclusions on the AAL- $\Lambda_s\text{CDM}$, a more rigorous and comprehensive analysis should be conducted by setting N_{eff} to the specific value of 3.294 in $\Lambda_s\text{CDM}$ model, as suggested by the AAL- $\Lambda_s\text{CDM}$ model, and then confronting it with the observational data using MCMC analysis. While this paper was nearing completion, a work confronting the AAL- $\Lambda_s\text{CDM}$ model, along with $\Lambda_s\text{CDM}$ and ΛCDM models, with observational data, appeared on arXiv. We refer the reader to Ref. [67] for further details on the observational analysis of the AAL- $\Lambda_s\text{CDM}$ model, which is dubbed as $\Lambda_s\text{CDM}^+$ in that paper. This stringy realization of the abrupt $\Lambda_s\text{CDM}$ model offers promising results both in fitting the data and resolving major cosmological tensions. It incorporates both pre- and post-recombination modifications to the standard ΛCDM model, namely, the rapid mirror AdS-dS transition in the late universe (at $z_\dagger \sim 2$) and an increased effective number of neutrino species, $\Delta N_{\text{eff}} \sim 0.25$. Notably, compared to the abrupt, $\Lambda_s\text{CDM}$ model, it predicts slightly higher H_0 values despite the slightly larger z_\dagger value they found. Specifically, they report $H_0 = 74.0 \text{ km s}^{-1} \text{ Mpc}^{-1}$ with $z_\dagger \sim 2.1$ in AAL- $\Lambda_s\text{CDM}$ and $H_0 = 73.4 \text{ km s}^{-1} \text{ Mpc}^{-1}$ with $z_\dagger \sim 1.9$ in $\Lambda_s\text{CDM}$, based on their dataset.

V. CONCLUSION

The $\Lambda_s\text{CDM}$ cosmology [59–61] extends the standard model of cosmology, the ΛCDM model, by promoting its positive cosmological constant (Λ) assumption to a rapidly sign-switching cosmological constant (Λ_s), namely, a rapid mirror AdS-dS transition, in the late universe, around $z_\dagger \sim 2$, as first conjectured in [58] based on findings in the graduated dark energy (gDE) model. In its simplest, idealized form, the abrupt $\Lambda_s\text{CDM}$ model [59–61] introduces z_\dagger , the redshift at which the mirror AdS-dS transition occurs instantaneously, as the only additional free parameter beyond the standard ΛCDM model. Detailed observational analyses of the abrupt $\Lambda_s\text{CDM}$ model have demonstrated its ability to address major cosmological tensions such as the H_0 , M_B , and S_8 tensions, as well as less significant discrepancies like $L_Y\text{-}\alpha$ and t_0 anomalies, simultaneously [59–61]. Recent theoretical advances regarding the potential physical mechanisms underlying a late-time mirror AdS-dS transition, such as those introduced in Refs. [62, 66] have propelled $\Lambda_s\text{CDM}$ cosmology beyond a phenomenological framework into a fully predictive physical cosmological model.

The standard $\Lambda_s\text{CDM}$ cosmology suggests a post-recombination modification to ΛCDM , leaving the pre-recombination universe as described in standard cosmology. Therefore, it is crucial to further investigate whether this framework indeed leaves the pre-combination universe unaltered if modifications related to early universe dynamics, such as variations in the number of neutrino species and the total mass of neutrinos, which are directly related to the standard model of particle physics, are allowed. In this paper, we have considered, for the first time, a two-parameter extension of the abrupt $\Lambda_s\text{CDM}$ model, as well as ΛCDM for comparison purposes. These extensions involve treating the effective number of relativistic neutrino species $N_{\text{eff}} = 3.044$ and a minimal mass $\sum m_\nu = 0.06 \text{ eV}$ of the SM of particle physics, inherent in the standard $\Lambda_s\text{CDM}$ and ΛCDM models, as free parameters to be predicted from cosmological observational analyses. We have first discussed the physical and cosmological implications of deviating N_{eff} and $\sum m_\nu$ from their standard values (see Section II). We then conducted observational analyses to constrain the free parameters in the extended models— $\Lambda_s\text{CDM} + N_{\text{eff}} + \sum m_\nu$ and $\Lambda\text{CDM} + N_{\text{eff}} + \sum m_\nu$ —using the Planck CMB, BAO (3D BAO), and alternative to this BAOtr (2D BAO), and PantheonPlus&SH0ES datasets (see Section III) and then discuss our findings in detail (see Section IV). Our approach presents one of the first/few examples of considering both late-time (introducing new physics operating in the post-recombination universe and deforming Hubble parameter) and early-time (introducing new physics operating in the pre-recombination universe and reducing the sound horizon) modifications proposed to address H_0 tension; see Refs. [49, 144, 208, 229–237]. This allowed us to assess whether data suggest late- or early-time modifications, or both (as suggested in [20]), to better fit the

TABLE III. We present the tensions of the predicted N_{eff} and Y_{p} values from the observational analyses with the $N_{\text{eff}}^{\text{AAL}} = 3.294$ ($\Delta N_{\text{eff}}^{\text{AAL}} = 0.25$) and $Y_{\text{p}}^{\text{AAL}} = 0.2512 \pm 0.0006$ (calculated semi-theoretically considering $\Delta N_{\text{eff}}^{\text{AAL}} = 0.25$) predicted by the theory realization of AdS-dS transition in the vacuum energy using the Casimir forces of fields inhabiting the bulk [66–68]. In the last two lines, we have compared the theoretical SBBN predictions of Y_{p} with the observationally obtained Y_{p} values for both models [228].

Dataset	Planck	Planck+BAO	Planck+BAOtr	Planck+BAO +PP&SH0ES	Planck+BAOtr +PP&SH0ES
Model	$\Lambda_{\text{s}}\text{CDM}+N_{\text{eff}}+\sum m_{\nu}$				
	$\Lambda\text{CDM}+N_{\text{eff}}+\sum m_{\nu}$				
N_{eff} (AAL)	2.0 σ	2.2 σ	1.7 σ	1.0 σ	1.3 σ
Y_{p} (AAL)	1.9 σ	2.2 σ	1.6 σ	1.0 σ	1.1 σ
$Y_{\text{p}}^{\text{SBBN}}$	0.7 σ	0.9 σ	0.3 σ	2.5 σ	0.5 σ
	0.8 σ	0.6 σ	0.6 σ	3.3 σ	3.3 σ

data, compared to ΛCDM , and address the cosmological tensions, particularly the H_0 tension, while remaining consistent with the SM of particle physics.

In the CMB-alone analysis, we have found no tension at all in any of the parameters of interest (namely, H_0 , M_B , S_8 , N_{eff} , Y_{p} , and ω_b) within the context of the $\Lambda_{\text{s}}\text{CDM}+N_{\text{eff}}+\sum m_{\nu}$ model. In contrast, for the $\Lambda\text{CDM}+N_{\text{eff}}+\sum m_{\nu}$ model, while the H_0 tension is only slightly alleviated to a 3.6 σ level, the so-called S_8 tension remains at a 3 σ level. N_{eff} values are found to be ~ 2.9 for both models, consistent within 1 σ with the SM of particle physics value of $N_{\text{eff}} = 3.044$. We also confronted both extended models with the combined Planck+BAO and Planck+BAO+PP&SH0ES datasets, as well as the combined Planck+BAOtr and Planck+BAOtr+PP&SH0ES datasets, considering BAOtr (2D BAO) data, which are less-model dependent, instead of the BAO (3D BAO). As anticipated, in the case of both Planck+BAO and Planck+BAO+PP&SH0ES, the extended $\Lambda_{\text{s}}\text{CDM}$ model approaches the extended ΛCDM model due to the opposition of Galaxy BAO data, pushing z_{\dagger} to higher values to give smaller H_0 . Therefore, for the combined Planck+BAO+PP&SH0ES, the moderate enhancement in H_0 within $\Lambda_{\text{s}}\text{CDM}+N_{\text{eff}}+\sum m_{\nu}$ is to some extent a result of $\Delta N_{\text{eff}} \sim 0.4$ rather than the effect of an efficient a mirror AdS-dS transition. Likewise, $\Lambda\text{CDM}+N_{\text{eff}}+\sum m_{\nu}$ model relaxes the H_0 tension through $\Delta N_{\text{eff}} \sim 0.5$. Unfortunately, this improvement in H_0 creates a new Y_{p} tension with astrophysical measurements of the primordial helium-4 abundances and demands new physics beyond the SM of particle physics. Additionally, the existing S_8 tension is worsened by the increased pre-recombination expansion in the $\Lambda\text{CDM}+N_{\text{eff}}+\sum m_{\nu}$ model.

On the other hand, we achieved a remarkable improvement in the fit to the data when we considered BAOtr instead of BAO in the analysis, resulting in no tension at all while simultaneously remaining fully consistent with the SM of particle physics using the $\Lambda_{\text{s}}\text{CDM}+N_{\text{eff}}+\sum m_{\nu}$ model. For the Planck+BAOtr and Planck+BAOtr+PP&SH0ES datasets, the H_0 tension is entirely eliminated, with the value $H_0 \approx 73 \text{ km s}^{-1} \text{ Mpc}^{-1}$ obtained in $\Lambda_{\text{s}}\text{CDM}+N_{\text{eff}}+\sum m_{\nu}$. Additionally, N_{eff} is constrained to be $N_{\text{eff}} \sim 3$ and $N_{\text{eff}} \sim 3.1$, respectively,

both of which are in agreement with $N_{\text{eff}} = 3.044$ at 1 σ . Nevertheless, even though $\Lambda\text{CDM}+N_{\text{eff}}+\sum m_{\nu}$ also resolves the H_0 tension, the model loses its coherence with the SM of particle physics and suffers from the same Y_{p} tension mentioned above because of $\Delta N_{\text{eff}} \sim 0.5$. An important realization at this point is that a post-recombination modification at $z \sim 1.6$ in the form of a rapidly sign-switching cosmological constant Λ_{s} , namely, a rapid mirror AdS-dS transition, is strongly favored over an early-time deformation of $H(z)$ induced by $\Delta N_{\text{eff}} > 0$, with the Bayesian evidence value of $\ln \mathcal{B}_{ij} \sim -11$.

In addition, the upper bounds on the sum of neutrino masses in the $\Lambda_{\text{s}}\text{CDM}+N_{\text{eff}}+\sum m_{\nu}$ model are about $\sum m_{\nu} \lesssim 0.50 \text{ eV}$, being consistent with the lower bounds provided by the neutrino oscillation experiments, i.e., $\sum m_{\nu} > 0.06 \text{ eV}$ (assuming the normal ordering) and $\sum m_{\nu} > 0.10 \text{ eV}$ (assuming the inverted ordering). These bounds help to remedy the S_8 tension by suppressing clustering σ_8 when matter density Ω_{m} is not sufficiently low, especially in cases where the model is subjected to Planck, Planck+BAO, Planck+BAO+PP&SH0ES datasets. However, the upper bounds placed on $\sum m_{\nu}$ using $\Lambda\text{CDM}+N_{\text{eff}}+\sum m_{\nu}$ are extremely tight, with $\sum m_{\nu} < 0.06 \text{ eV}$ for Planck+BAOtr and Planck+BAOtr+PP&SH0ES, and $\sum m_{\nu} < 0.13 \text{ eV}$ for Planck+BAO and Planck+BAO+PP&SH0ES. Consequently, σ_8 values preferred by these datasets are typically larger in $\Lambda\text{CDM}+N_{\text{eff}}+\sum m_{\nu}$ than in $\Lambda_{\text{s}}\text{CDM}+N_{\text{eff}}+\sum m_{\nu}$, partially hampering the alleviation of the S_8 tension. We also briefly commented on how the two-parameter extensions $\Lambda_{\text{s}}\text{CDM}+N_{\text{eff}}+\sum m_{\nu}$ and $\Lambda\text{CDM}+N_{\text{eff}}+\sum m_{\nu}$ compare to their respective baseline models—namely, the abrupt $\Lambda_{\text{s}}\text{CDM}$ and standard ΛCDM models—as well as to other widely studied frameworks (including also examples proposed to address the H_0 and S_8 tensions) that have been explored by extending their base versions to incorporate new early-time degrees of freedom, particularly by allowing neutrino properties to deviate from those predicted by the SM of particle physics. Our analysis demonstrates that the $\Lambda_{\text{s}}\text{CDM}$ framework, encompassing both its base form and the $N_{\text{eff}} + \sum m_{\nu}$ extension, significantly outperforms the standard ΛCDM framework, as well as the $w\text{CDM}$ and $w_0w_a\text{CDM}$ frame-

works, by exhibiting greater stability in predicting neutrino properties consistent with the standard model of particle physics, while simultaneously maintaining its success in alleviating major cosmological tensions. And, in the last section, we evaluated the $\Delta N_{\text{eff}} \approx 0.25$ prediction of the AAL- Λ_s CDM model [66–68] in the extended Λ_s CDM studied in this paper and detected no serious incompatibility between the two models.

Furthermore, around the appearance of this work on arXiv, the analyses [160, 224, 238–242] combining CMB data with the recent DESI BAO measurements have revealed that when the neutrino mass is treated as a free parameter within the Λ CDM framework, the data favor values of $\sum m_\nu$ below the minimum inferred from neutrino flavor oscillation experiments. This preference for negative effective neutrino masses persists in extensions such as $w_0 w_a$ CDM and mirage dark energy models (a specific case of $w_0 w_a$ CDM), especially when SNIa compilations like the Pantheon+ data are included in the analysis [240]. Specifically, for the Λ CDM framework using Planck+ACT+DESI BAO data, the best-fit value of the effective neutrino mass parameter $\sum m_\nu$ is negative and in tension at the 3σ level with constraints from neutrino oscillation experiments [240]. This result indicates another anomaly within the Λ CDM framework, as negative neutrino masses are unphysical, while the theoretical lower bound is $\sum m_\nu > 0.06$ eV based on oscillation data. In our analyses, where we restrict $\sum m_\nu$ to positive values, the Λ CDM+ N_{eff} + $\sum m_\nu$ model tends to predict upper bounds that approach this theoretical lower limit, even reaching it when BAOtr data are involved. This suggests that if negative neutrino masses were permitted, the data we used, particularly when BAOtr data are included, might also favor such unphysical values, highlighting another potential discrepancy within the Λ CDM framework. In contrast, the Λ_s CDM+ N_{eff} + $\sum m_\nu$ model consistently predicts realistic upper bounds on the sum of neutrino masses, maintaining $\sum m_\nu \lesssim 0.4$ eV across our datasets. This indicates that the Λ_s CDM model may offer a promising solution to this new potential anomaly concerning neutrino mass. A detailed investigation into this matter is currently underway and will be presented elsewhere.

These findings further highlight the robustness of the Λ_s CDM framework in addressing emerging anomalies in cosmology. As a final remark, we note that the extensive literature attempting to address the shortcomings of the standard cosmological model by proposing modifications spanning the entire or a long history of the universe often includes regimes that are inaccessible with direct observational methods. This broad approach can be akin to looking for a needle in a haystack when trying to resolve issues that arise within the Λ CDM framework. Therefore, it might be more effective to narrow down the

time/redshift scale in which a more complete cosmological framework can be sought, guided by the observational data, as suggested in Ref. [21]. This focused approach could help localize the possible missing physics, ideally by introducing minimal (though not necessarily trivial) modifications, aiding in a better understanding of the universe. Models possessing this property would allow for further testing via new and independent methods and ideally direct observations with current or future experiments. Certain extensions of the Λ_s CDM model, introducing modifications on top of its directly detectable new physics around $z \sim 2$, such as Λ_s CDM+ N_{eff} + $\sum m_\nu$ studied in the current work, enable us to test whether the data prefer pre- or post-recombination new physics, or both (as suggested in Ref. [20]). Our work here provides a compelling example, highlighting the potential of new physics in the late universe around $z \sim 2$ against the pre-recombination new physics closely related to the SM of particle physics. This late-time AdS-dS transition era around $z \sim 2$ remains accessible to direct observations in principle, in contrast to pre-recombination epochs where we mainly rely on indirect observations. Thus, it would be worthwhile to further investigate the Λ_s CDM model, as well as its standard extensions similar to the ones applied to the Λ CDM model as we have done here, and, perhaps even better, its realizations based on different physical theories—which usually come with different types of corrections on top of the simplest abrupt Λ_s CDM model, see, e.g., Ref. [62, 63, 66, 67]—can help in our quest to establish a physical cosmology better at describing cosmological phenomena than today’s standard model of cosmology, i.e., the Λ CDM model.

ACKNOWLEDGMENTS

The authors thank Luis A. Anchordoqui for fruitful discussions. A.Y. is supported by a Senior Research Fellowship (CSIR/UGC Ref. No. 201610145543) from the University Grants Commission, Govt. of India. S.K. gratefully acknowledges the support of Startup Research Grant from Plaksha University (File No. OOR/PU-SRG/2023-24/08), and Core Research Grant from Science and Engineering Research Board (SERB), Govt. of India (File No. CRG/2021/004658). Ö.A. acknowledges the support of the Turkish Academy of Sciences in the scheme of the Outstanding Young Scientist Award (TÜBA-GEBİP). This study was supported by Scientific and Technological Research Council of Turkey (TUBITAK) under the Grant Number 122F124. The authors thank TUBITAK for their support.

[1] A. G. Riess *et al.* (Supernova Search Team), *Astron. J.* **116**, 1009 (1998), arXiv:astro-ph/9805201.

[2] S. Perlmutter *et al.* (Supernova Cosmology Project),

- Astrophys. J.* **517**, 565 (1999), [arXiv:astro-ph/9812133](#).
- [3] N. Aghanim *et al.* (Planck), *Astron. Astrophys.* **641**, A6 (2020), [Erratum: *Astron. Astrophys.* 652, C4 (2021)], [arXiv:1807.06209 \[astro-ph.CO\]](#).
- [4] F. Bernardeau, S. Colombi, E. Gaztanaga, and R. Scoccimarro, *Phys. Rept.* **367**, 1 (2002), [arXiv:astro-ph/0112551](#).
- [5] S. Aiola *et al.* (ACT), *JCAP* **12**, 047 (2020), [arXiv:2007.07288 \[astro-ph.CO\]](#).
- [6] S. Alam *et al.* (eBOSS), *Phys. Rev. D* **103**, 083533 (2021), [arXiv:2007.08991 \[astro-ph.CO\]](#).
- [7] L. Balkenhol *et al.* (SPT-3G), *Phys. Rev. D* **104**, 083509 (2021), [arXiv:2103.13618 \[astro-ph.CO\]](#).
- [8] T. M. C. Abbott *et al.* (DES), *Phys. Rev. D* **107**, 083504 (2023), [arXiv:2207.05766 \[astro-ph.CO\]](#).
- [9] A. G. Adame *et al.* (DESI), [arXiv:2404.03002 \(2024\)](#), [arXiv:2404.03002 \[astro-ph.CO\]](#).
- [10] P. Bull *et al.*, *Phys. Dark Univ.* **12**, 56 (2016), [arXiv:1512.05356 \[astro-ph.CO\]](#).
- [11] W. L. Freedman, *Nature Astron.* **1**, 0121 (2017), [arXiv:1706.02739 \[astro-ph.CO\]](#).
- [12] J. S. Bullock and M. Boylan-Kolchin, *Ann. Rev. Astron. Astrophys.* **55**, 343 (2017), [arXiv:1707.04256 \[astro-ph.CO\]](#).
- [13] E. Di Valentino, *Nature Astron.* **1**, 569 (2017), [arXiv:1709.04046 \[physics.pop-ph\]](#).
- [14] E. Di Valentino *et al.*, *Astropart. Phys.* **131**, 102606 (2021), [arXiv:2008.11283 \[astro-ph.CO\]](#).
- [15] E. Di Valentino *et al.*, *Astropart. Phys.* **131**, 102605 (2021), [arXiv:2008.11284 \[astro-ph.CO\]](#).
- [16] E. Di Valentino *et al.*, *Astropart. Phys.* **131**, 102604 (2021), [arXiv:2008.11285 \[astro-ph.CO\]](#).
- [17] E. Di Valentino *et al.*, *Astropart. Phys.* **131**, 102607 (2021), [arXiv:2008.11286 \[astro-ph.CO\]](#).
- [18] L. Perivolaropoulos and F. Skara, *New Astron. Rev.* **95**, 101659 (2022), [arXiv:2105.05208 \[astro-ph.CO\]](#).
- [19] E. Abdalla *et al.*, *JHEAp* **34**, 49 (2022), [arXiv:2203.06142 \[astro-ph.CO\]](#).
- [20] S. Vagnozzi, *Universe* **9**, 393 (2023), [arXiv:2308.16628 \[astro-ph.CO\]](#).
- [21] O. Akarsu, E. O. Colgáin, A. A. Sen, and M. M. Sheikh-Jabbari, (2024), [arXiv:2402.04767 \[astro-ph.CO\]](#).
- [22] K. C. Wong *et al.*, *Mon. Not. Roy. Astron. Soc.* **498**, 1420 (2020), [arXiv:1907.04869 \[astro-ph.CO\]](#).
- [23] A. G. Riess, *Nature Rev. Phys.* **2**, 10 (2019), [arXiv:2001.03624 \[astro-ph.CO\]](#).
- [24] E. Di Valentino, O. Mena, S. Pan, L. Visinelli, W. Yang, A. Melchiorri, D. F. Mota, A. G. Riess, and J. Silk, *Class. Quant. Grav.* **38**, 153001 (2021), [arXiv:2103.01183 \[astro-ph.CO\]](#).
- [25] A. G. Riess *et al.*, *Astrophys. J. Lett.* **934**, L7 (2022), [arXiv:2112.04510 \[astro-ph.CO\]](#).
- [26] L. Breuval, A. G. Riess, S. Casertano, W. Yuan, L. M. Macri, M. Romaniello, Y. S. Murakami, D. Scolnic, G. S. Anand, and I. Soszyński, [arXiv:2404.08038 \(2024\)](#), [arXiv:2404.08038 \[astro-ph.CO\]](#).
- [27] S. A. Uddin *et al.*, [arXiv:2308.01875 \(2023\)](#), [arXiv:2308.01875 \[astro-ph.CO\]](#).
- [28] R. C. Nunes and S. Vagnozzi, *Mon. Not. Roy. Astron. Soc.* **505**, 5427 (2021), [arXiv:2106.01208 \[astro-ph.CO\]](#).
- [29] S. A. Adil, O. Akarsu, M. Malekjani, E. O. Colgáin, S. Pourojaghi, A. A. Sen, and M. M. Sheikh-Jabbari, *Mon. Not. Roy. Astron. Soc.* **528**, L20 (2023), [arXiv:2303.06928 \[astro-ph.CO\]](#).
- [30] O. Akarsu, E. O. Colgáin, A. A. Sen, and M. M. Sheikh-Jabbari, (2024), [arXiv:2410.23134 \[astro-ph.CO\]](#).
- [31] M. Asgari *et al.* (KiDS), *Astron. Astrophys.* **645**, A104 (2021), [arXiv:2007.15633 \[astro-ph.CO\]](#).
- [32] L. F. Secco *et al.* (DES), *Phys. Rev. D* **105**, 023515 (2022), [arXiv:2105.13544 \[astro-ph.CO\]](#).
- [33] T. Karwal and M. Kamionkowski, *Phys. Rev. D* **94**, 103523 (2016), [arXiv:1608.01309 \[astro-ph.CO\]](#).
- [34] V. Poulin, T. L. Smith, T. Karwal, and M. Kamionkowski, *Phys. Rev. Lett.* **122**, 221301 (2019), [arXiv:1811.04083 \[astro-ph.CO\]](#).
- [35] V. Poulin, T. L. Smith, D. Grin, T. Karwal, and M. Kamionkowski, *Phys. Rev. D* **98**, 083525 (2018), [arXiv:1806.10608 \[astro-ph.CO\]](#).
- [36] P. Agrawal, F.-Y. Cyr-Racine, D. Pinner, and L. Randall, *Phys. Dark Univ.* **42**, 101347 (2023), [arXiv:1904.01016 \[astro-ph.CO\]](#).
- [37] M. Kamionkowski and A. G. Riess, *Ann. Rev. Nucl. Part. Sci.* **73**, 153 (2023), [arXiv:2211.04492 \[astro-ph.CO\]](#).
- [38] S. D. Odintsov, V. K. Oikonomou, and G. S. Sharov, *Phys. Lett. B* **843**, 137988 (2023), [arXiv:2305.17513 \[gr-qc\]](#).
- [39] F. Niedermann and M. S. Sloth, *Phys. Rev. D* **103**, L041303 (2021), [arXiv:1910.10739 \[astro-ph.CO\]](#).
- [40] J. S. Cruz, F. Niedermann, and M. S. Sloth, *JCAP* **11**, 033 (2023), [arXiv:2305.08895 \[astro-ph.CO\]](#).
- [41] F. Niedermann and M. S. Sloth, (2023), [arXiv:2307.03481 \[hep-ph\]](#).
- [42] G. Ye and Y.-S. Piao, *Phys. Rev. D* **101**, 083507 (2020), [arXiv:2001.02451 \[astro-ph.CO\]](#).
- [43] G. Ye and Y.-S. Piao, *Phys. Rev. D* **102**, 083523 (2020), [arXiv:2008.10832 \[astro-ph.CO\]](#).
- [44] G. Ye, J. Zhang, and Y.-S. Piao, *Phys. Lett. B* **839**, 137770 (2023), [arXiv:2107.13391 \[astro-ph.CO\]](#).
- [45] A. G. Riess *et al.*, *Astrophys. J.* **826**, 56 (2016), [arXiv:1604.01424 \[astro-ph.CO\]](#).
- [46] S. Vagnozzi, *Phys. Rev. D* **102**, 023518 (2020), [arXiv:1907.07569 \[astro-ph.CO\]](#).
- [47] V. V. Flambaum and I. B. Samsonov, *Phys. Rev. D* **100**, 063541 (2019), [arXiv:1908.09432 \[astro-ph.CO\]](#).
- [48] O. Seto and Y. Toda, *Phys. Rev. D* **103**, 123501 (2021), [arXiv:2101.03740 \[astro-ph.CO\]](#).
- [49] A. Reeves, L. Herold, S. Vagnozzi, B. D. Sherwin, and E. G. M. Ferreira, *Mon. Not. Roy. Astron. Soc.* **520**, 3688 (2023), [arXiv:2207.01501 \[astro-ph.CO\]](#).
- [50] M. Rossi, M. Ballardini, M. Braglia, F. Finelli, D. Paoletti, A. A. Starobinsky, and C. Umiltà, *Phys. Rev. D* **100**, 103524 (2019), [arXiv:1906.10218 \[astro-ph.CO\]](#).
- [51] M. Braglia, M. Ballardini, W. T. Emond, F. Finelli, A. E. Gumrukcuoglu, K. Koyama, and D. Paoletti, *Phys. Rev. D* **102**, 023529 (2020), [arXiv:2004.11161 \[astro-ph.CO\]](#).
- [52] T. Adi and E. D. Kovetz, *Phys. Rev. D* **103**, 023530 (2021), [arXiv:2011.13853 \[astro-ph.CO\]](#).
- [53] M. Braglia, M. Ballardini, F. Finelli, and K. Koyama, *Phys. Rev. D* **103**, 043528 (2021), [arXiv:2011.12934 \[astro-ph.CO\]](#).
- [54] M. Ballardini, M. Braglia, F. Finelli, D. Paoletti, A. A. Starobinsky, and C. Umiltà, *JCAP* **10**, 044 (2020), [arXiv:2004.14349 \[astro-ph.CO\]](#).
- [55] G. Franco Abellán, M. Braglia, M. Ballardini, F. Finelli, and V. Poulin, *JCAP* **12**, 017 (2023), [arXiv:2308.12345 \[astro-ph.CO\]](#).
- [56] M. Petronikolou and E. N. Saridakis, *Universe* **9**, 397 (2023), [arXiv:2308.16044 \[gr-qc\]](#).

- [57] D. K. Hazra, A. Antony, and A. Shafieloo, *JCAP* **08**, 063 (2022), [arXiv:2201.12000 \[astro-ph.CO\]](#).
- [58] O. Akarsu, J. D. Barrow, L. A. Escamilla, and J. A. Vazquez, *Phys. Rev. D* **101**, 063528 (2020), [arXiv:1912.08751 \[astro-ph.CO\]](#).
- [59] O. Akarsu, S. Kumar, E. Özüiker, and J. A. Vazquez, *Phys. Rev. D* **104**, 123512 (2021), [arXiv:2108.09239 \[astro-ph.CO\]](#).
- [60] O. Akarsu, S. Kumar, E. Özüiker, J. A. Vazquez, and A. Yadav, *Phys. Rev. D* **108**, 023513 (2023), [arXiv:2211.05742 \[astro-ph.CO\]](#).
- [61] O. Akarsu, E. Di Valentino, S. Kumar, R. C. Nunes, J. A. Vazquez, and A. Yadav, (2023), [arXiv:2307.10899 \[astro-ph.CO\]](#).
- [62] O. Akarsu, A. De Felice, E. Di Valentino, S. Kumar, R. C. Nunes, E. Ozulker, J. A. Vazquez, and A. Yadav, (2024), [arXiv:2402.07716 \[astro-ph.CO\]](#).
- [63] O. Akarsu, A. De Felice, E. Di Valentino, S. Kumar, R. C. Nunes, E. Ozulker, J. A. Vazquez, and A. Yadav, 2406.06389 (2024), [arXiv:2406.07526 \[astro-ph.CO\]](#).
- [64] A. De Felice, A. Doll, and S. Mukohyama, *JCAP* **09**, 034 (2020), [arXiv:2004.12549 \[gr-qc\]](#).
- [65] A. De Felice, S. Mukohyama, and M. C. Pookkillath, *Phys. Lett. B* **816**, 136201 (2021), [Erratum: *Phys. Lett. B* 818, 136364 (2021)], [arXiv:2009.08718 \[astro-ph.CO\]](#).
- [66] L. A. Anchordoqui, I. Antoniadis, and D. Lust, (2023), [arXiv:2312.12352 \[hep-th\]](#).
- [67] L. A. Anchordoqui, I. Antoniadis, D. Lust, N. T. Noble, and J. F. Soriano, *Phys. Dark Univ.* **46**, 101715 (2024), [arXiv:2404.17334 \[astro-ph.CO\]](#).
- [68] L. A. Anchordoqui, I. Antoniadis, D. Bielli, A. Chatrabhuti, and H. Isono, (2024), [arXiv:2410.18649 \[hep-th\]](#).
- [69] E. Di Valentino, A. Mukherjee, and A. A. Sen, *Entropy* **23**, 404 (2021), [arXiv:2005.12587 \[astro-ph.CO\]](#).
- [70] G. Alestas, L. Kazantzidis, and L. Perivolaropoulos, *Phys. Rev. D* **101**, 123516 (2020), [arXiv:2004.08363 \[astro-ph.CO\]](#).
- [71] G. Alestas, L. Kazantzidis, and L. Perivolaropoulos, *Phys. Rev. D* **103**, 083517 (2021), [arXiv:2012.13932 \[astro-ph.CO\]](#).
- [72] M. R. Gangopadhyay, S. K. J. Pacif, M. Sami, and M. K. Sharma, *Universe* **9**, 83 (2023), [arXiv:2211.12041 \[gr-qc\]](#).
- [73] S. Basilakos, A. Lymperis, M. Petronikolou, and E. N. Saridakis, *Eur. Phys. J. C* **84**, 297 (2024), [arXiv:2308.01200 \[gr-qc\]](#).
- [74] S. A. Adil, O. Akarsu, E. Di Valentino, R. C. Nunes, E. Özüiker, A. A. Sen, and E. Specogna, *Phys. Rev. D* **109**, 023527 (2024), [arXiv:2306.08046 \[astro-ph.CO\]](#).
- [75] M. R. Gangopadhyay, M. Sami, and M. K. Sharma, *Phys. Rev. D* **108**, 103526 (2023), [arXiv:2303.07301 \[astro-ph.CO\]](#).
- [76] L. Visinelli, S. Vagnozzi, and U. Danielsson, *Symmetry* **11**, 1035 (2019), [arXiv:1907.07953 \[astro-ph.CO\]](#).
- [77] R. Calderón, R. Gannouji, B. L'Huilier, and D. Polarski, *Phys. Rev. D* **103**, 023526 (2021), [arXiv:2008.10237 \[astro-ph.CO\]](#).
- [78] K. Dutta, Ruchika, A. Roy, A. A. Sen, and M. M. Sheikh-Jabbari, *Gen. Rel. Grav.* **52**, 15 (2020), [arXiv:1808.06623 \[astro-ph.CO\]](#).
- [79] A. A. Sen, S. A. Adil, and S. Sen, *Mon. Not. Roy. Astron. Soc.* **518**, 1098 (2022), [arXiv:2112.10641 \[astro-ph.CO\]](#).
- [80] S. Kumar and R. C. Nunes, *Phys. Rev. D* **96**, 103511 (2017), [arXiv:1702.02143 \[astro-ph.CO\]](#).
- [81] E. Di Valentino, A. Melchiorri, and O. Mena, *Phys. Rev. D* **96**, 043503 (2017), [arXiv:1704.08342 \[astro-ph.CO\]](#).
- [82] W. Yang, A. Mukherjee, E. Di Valentino, and S. Pan, *Phys. Rev. D* **98**, 123527 (2018), [arXiv:1809.06883 \[astro-ph.CO\]](#).
- [83] S. Pan, W. Yang, E. Di Valentino, E. N. Saridakis, and S. Chakraborty, *Phys. Rev. D* **100**, 103520 (2019), [arXiv:1907.07540 \[astro-ph.CO\]](#).
- [84] S. Kumar, R. C. Nunes, and S. K. Yadav, *Eur. Phys. J. C* **79**, 576 (2019), [arXiv:1903.04865 \[astro-ph.CO\]](#).
- [85] E. Di Valentino, A. Melchiorri, O. Mena, and S. Vagnozzi, *Phys. Rev. D* **101**, 063502 (2020), [arXiv:1910.09853 \[astro-ph.CO\]](#).
- [86] E. Di Valentino, A. Melchiorri, O. Mena, and S. Vagnozzi, *Phys. Dark Univ.* **30**, 100666 (2020), [arXiv:1908.04281 \[astro-ph.CO\]](#).
- [87] M. Lucca and D. C. Hooper, *Phys. Rev. D* **102**, 123502 (2020), [arXiv:2002.06127 \[astro-ph.CO\]](#).
- [88] A. Gómez-Valent, V. Pettorino, and L. Amendola, *Phys. Rev. D* **101**, 123513 (2020), [arXiv:2004.00610 \[astro-ph.CO\]](#).
- [89] S. Kumar, *Phys. Dark Univ.* **33**, 100862 (2021), [arXiv:2102.12902 \[astro-ph.CO\]](#).
- [90] R. C. Nunes, S. Vagnozzi, S. Kumar, E. Di Valentino, and O. Mena, *Phys. Rev. D* **105**, 123506 (2022), [arXiv:2203.08093 \[astro-ph.CO\]](#).
- [91] A. Bernui, E. Di Valentino, W. Giarè, S. Kumar, and R. C. Nunes, *Phys. Rev. D* **107**, 103531 (2023), [arXiv:2301.06097 \[astro-ph.CO\]](#).
- [92] L. A. Escamilla, O. Akarsu, E. Di Valentino, and J. A. Vazquez, *JCAP* **11**, 051 (2023), [arXiv:2305.16290 \[astro-ph.CO\]](#).
- [93] J. Solà Peracaula, A. Gómez-Valent, J. de Cruz Perez, and C. Moreno-Pulido, *EPL* **134**, 19001 (2021), [arXiv:2102.12758 \[astro-ph.CO\]](#).
- [94] J. Sola Peracaula, A. Gomez-Valent, J. de Cruz Perez, and C. Moreno-Pulido, *Universe* **9**, 262 (2023), [arXiv:2304.11157 \[astro-ph.CO\]](#).
- [95] J. Sola Peracaula, *Phil. Trans. Roy. Soc. Lond. A* **380**, 20210182 (2022), [arXiv:2203.13757 \[gr-qc\]](#).
- [96] X. Li and A. Shafieloo, *Astrophys. J. Lett.* **883**, L3 (2019), [arXiv:1906.08275 \[astro-ph.CO\]](#).
- [97] V. Marra and L. Perivolaropoulos, *Phys. Rev. D* **104**, L021303 (2021), [arXiv:2102.06012 \[astro-ph.CO\]](#).
- [98] G. Alestas, I. Antoniou, and L. Perivolaropoulos, *Universe* **7**, 366 (2021), [arXiv:2104.14481 \[astro-ph.CO\]](#).
- [99] G. Alestas, D. Camarena, E. Di Valentino, L. Kazantzidis, V. Marra, S. Nesseris, and L. Perivolaropoulos, *Phys. Rev. D* **105**, 063538 (2022), [arXiv:2110.04336 \[astro-ph.CO\]](#).
- [100] L. Perivolaropoulos and F. Skara, *Phys. Rev. D* **104**, 123511 (2021), [arXiv:2109.04406 \[astro-ph.CO\]](#).
- [101] S. Pan, O. Seto, T. Takahashi, and Y. Toda, (2023), [arXiv:2312.15435 \[astro-ph.CO\]](#).
- [102] K. Naidoo, M. Jaber, W. A. Hellwing, and M. Bilicki, *Phys. Rev. D* **109**, 083511 (2024), [arXiv:2209.08102 \[astro-ph.CO\]](#).
- [103] A. Perez, D. Sudarsky, and E. Wilson-Ewing, *Gen. Rel. Grav.* **53**, 7 (2021), [arXiv:2001.07536 \[astro-ph.CO\]](#).
- [104] G. Acquaviva, O. Akarsu, N. Katirci, and J. A. Vazquez, *Phys. Rev. D* **104**, 023505 (2021), [arXiv:2104.02623 \[astro-ph.CO\]](#).
- [105] E. Ozulker, *Phys. Rev. D* **106**, 063509 (2022),

- arXiv:2203.04167 [astro-ph.CO].
- [106] S. Di Gennaro and Y. C. Ong, *Universe* **8**, 541 (2022), arXiv:2205.09311 [gr-qc].
- [107] H. Moshafi, H. Firouzjahi, and A. Talebian, *Astrophys. J.* **940**, 121 (2022), arXiv:2208.05583 [astro-ph.CO].
- [108] A. van de Venn, D. Vasak, J. Kirsch, and J. Struckmeier, *Eur. Phys. J. C* **83**, 288 (2023), arXiv:2211.11868 [gr-qc].
- [109] Y. C. Ong, *Universe* **9**, 437 (2023), arXiv:2212.04429 [gr-qc].
- [110] Y. Tiwari, B. Ghosh, and R. K. Jain, *Eur. Phys. J. C* **84**, 220 (2024), arXiv:2301.09382 [astro-ph.CO].
- [111] J. A. Vázquez, D. Tamayo, G. Garcia-Arroyo, I. Gómez-Vargas, I. Quiros, and A. A. Sen, *Phys. Rev. D* **109**, 023511 (2024), arXiv:2305.11396 [astro-ph.CO].
- [112] S. A. Adil, U. Mukhopadhyay, A. A. Sen, and S. Vagnozzi, *JCAP* **10**, 072 (2023), arXiv:2307.12763 [astro-ph.CO].
- [113] E. A. Paraskevas and L. Perivolaropoulos, 2308.07046 (2023), arXiv:2308.07046 [astro-ph.CO].
- [114] R. Y. Wen, L. T. Hergt, N. Afshordi, and D. Scott, *JCAP* **03**, 045 (2024), arXiv:2311.03028 [astro-ph.CO].
- [115] N. Menci, S. A. Adil, U. Mukhopadhyay, A. A. Sen, and S. Vagnozzi, 2404.15232 (2024), arXiv:2401.12659 [astro-ph.CO].
- [116] A. Gomez-Valent and J. Solà Peracaula, *Astrophys. J.* **975**, 64 (2024), arXiv:2404.18845 [astro-ph.CO].
- [117] A. D. Felice, S. Kumar, S. Mukohyama, and R. C. Nunes, *Journal of Cosmology and Astroparticle Physics* **2024**, 013 (2024).
- [118] M. T. Manoharan, *Eur. Phys. J. C* **84**, 552 (2024).
- [119] S. Dwivedi and M. Högås, (2024), arXiv:2407.04322 [astro-ph.CO].
- [120] O. Akarsu, B. Bulduk, A. De Felice, N. Katırcı, and N. M. Uzun, (2024), arXiv:2410.23068 [gr-qc].
- [121] V. Sahni, A. Shafieloo, and A. A. Starobinsky, *Astrophys. J. Lett.* **793**, L40 (2014), arXiv:1406.2209 [astro-ph.CO].
- [122] E. Aubourg *et al.* (BOSS), *Phys. Rev. D* **92**, 123516 (2015), arXiv:1411.1074 [astro-ph.CO].
- [123] V. Poulin, K. K. Boddy, S. Bird, and M. Kamionkowski, *Phys. Rev. D* **97**, 123504 (2018), arXiv:1803.02474 [astro-ph.CO].
- [124] Y. Wang, L. Pogosian, G.-B. Zhao, and A. Zucca, *Astrophys. J. Lett.* **869**, L8 (2018), arXiv:1807.03772 [astro-ph.CO].
- [125] A. Bonilla, S. Kumar, and R. C. Nunes, *Eur. Phys. J. C* **81**, 127 (2021), arXiv:2011.07140 [astro-ph.CO].
- [126] L. A. Escamilla and J. A. Vazquez, *Eur. Phys. J. C* **83**, 251 (2023), arXiv:2111.10457 [astro-ph.CO].
- [127] R. C. Bernardo, D. Grandón, J. Said Levi, and V. H. Cárdenas, *Phys. Dark Univ.* **36**, 101017 (2022), arXiv:2111.08289 [astro-ph.CO].
- [128] O. Akarsu, E. O. Colgain, E. Özulker, S. Thakur, and L. Yin, *Phys. Rev. D* **107**, 123526 (2023), arXiv:2207.10609 [astro-ph.CO].
- [129] R. C. Bernardo, D. Grandón, J. Levi Said, and V. H. Cárdenas, *Phys. Dark Univ.* **40**, 101213 (2023), arXiv:2211.05482 [astro-ph.CO].
- [130] M. Malekjani, R. M. Conville, E. O. Colgáin, S. Pourojaghi, and M. M. Sheikh-Jabbari, *Eur. Phys. J. C* **84**, 317 (2024), arXiv:2301.12725 [astro-ph.CO].
- [131] A. Gómez-Valent, A. Favale, M. Migliaccio, and A. A. Sen, *Phys. Rev. D* **109**, 023525 (2024), arXiv:2309.07795 [astro-ph.CO].
- [132] R. Medel-Esquível, I. Gómez-Vargas, A. A. M. Sánchez, R. García-Salcedo, and J. Alberto Vázquez, *Universe* **10**, 11 (2024), arXiv:2311.05699 [astro-ph.CO].
- [133] R. Calderon *et al.* (DESI), 2405.04216 (2024), arXiv:2405.04216 [astro-ph.CO].
- [134] D. Bousis and L. Perivolaropoulos, 2405.07039 (2024), arXiv:2405.07039 [astro-ph.CO].
- [135] H. Wang, Z.-Y. Peng, and Y.-S. Piao, 2406.03395 (2024), arXiv:2406.03395 [astro-ph.CO].
- [136] E. O. Colgáin, S. Pourojaghi, and M. M. Sheikh-Jabbari, 2406.06389 (2024), arXiv:2406.06389 [astro-ph.CO].
- [137] M. A. Sabogal, O. Akarsu, A. Bonilla, E. Di Valentino, and R. C. Nunes, arXiv:2407.04223 (2024), arXiv:2407.04223 [astro-ph.CO].
- [138] L. A. Escamilla, E. Özulker, O. Akarsu, E. Di Valentino, and J. A. Vázquez, (2024), arXiv:2408.12516 [astro-ph.CO].
- [139] T. L. Smith, V. Poulin, and M. A. Amin, *Phys. Rev. D* **101**, 063523 (2020), arXiv:1908.06995 [astro-ph.CO].
- [140] L. Herold and E. G. M. Ferreira, *Phys. Rev. D* **108**, 043513 (2023), arXiv:2210.16296 [astro-ph.CO].
- [141] K. Jedamzik, L. Pogosian, and G.-B. Zhao, *Commun. in Phys.* **4**, 123 (2021), arXiv:2010.04158 [astro-ph.CO].
- [142] V. Poulin, T. L. Smith, and T. Karwal, *Phys. Dark Univ.* **42**, 101348 (2023), arXiv:2302.09032 [astro-ph.CO].
- [143] S. Vagnozzi, *Phys. Rev. D* **104**, 063524 (2021), arXiv:2105.10425 [astro-ph.CO].
- [144] W. Yang, E. Di Valentino, S. Pan, and O. Mena, *Phys. Dark Univ.* **31**, 100762 (2021), arXiv:2007.02927 [astro-ph.CO].
- [145] R. N. Mohapatra *et al.*, *Rept. Prog. Phys.* **70**, 1757 (2007), arXiv:hep-ph/0510213.
- [146] E. Di Valentino, S. Gariazzo, and O. Mena, arXiv:2404.19322 (2024), arXiv:2404.19322 [astro-ph.CO].
- [147] C. D. Kreisch, F.-Y. Cyr-Racine, and O. Doré, *Phys. Rev. D* **101**, 123505 (2020), arXiv:1902.00534 [astro-ph.CO].
- [148] E. Di Valentino, W. Giarè, A. Melchiorri, and J. Silk, *Phys. Rev. D* **106**, 103506 (2022), arXiv:2209.12872 [astro-ph.CO].
- [149] E. di Valentino, S. Gariazzo, and O. Mena, *Phys. Rev. D* **106**, 043540 (2022), arXiv:2207.05167 [astro-ph.CO].
- [150] M. Forconi, E. Di Valentino, A. Melchiorri, and S. Pan, *Phys. Rev. D* **109**, 123532 (2024), arXiv:2311.04038 [astro-ph.CO].
- [151] S. Safi, M. Farhang, O. Mena, and E. Di Valentino, arXiv:2404.01457 (2024), arXiv:2404.01457 [astro-ph.CO].
- [152] S. Vagnozzi, E. Giusarma, O. Mena, K. Freese, M. Gerbino, S. Ho, and M. Lattanzi, *Phys. Rev. D* **96**, 123503 (2017), arXiv:1701.08172 [astro-ph.CO].
- [153] S. Vagnozzi, S. Dhawan, M. Gerbino, K. Freese, A. Goobar, and O. Mena, *Phys. Rev. D* **98**, 083501 (2018), arXiv:1801.08553 [astro-ph.CO].
- [154] E. Giusarma, S. Vagnozzi, S. Ho, S. Ferraro, K. Freese, R. Kamen-Rubio, and K.-B. Luk, *Phys. Rev. D* **98**, 123526 (2018), arXiv:1802.08694 [astro-ph.CO].
- [155] S. Roy Choudhury and S. Hannestad, *JCAP* **07**, 037 (2020), arXiv:1907.12598 [astro-ph.CO].
- [156] E. Di Valentino, S. Gariazzo, and O. Mena, *Phys. Rev. D* **104**, 083504 (2021), arXiv:2106.15267 [astro-ph.CO].

- [157] E. Di Valentino and A. Melchiorri, *Astrophys. J. Lett.* **931**, L18 (2022), arXiv:2112.02993 [astro-ph.CO].
- [158] I. Tanseri, S. Hagstotz, S. Vagnozzi, E. Giusarri, and K. Freese, *JHEAp* **36**, 1 (2022), arXiv:2207.01913 [astro-ph.CO].
- [159] E. Di Valentino, S. Gariazzo, W. Giarè, and O. Mena, *Phys. Rev. D* **108**, 083509 (2023), arXiv:2305.12989 [astro-ph.CO].
- [160] D. Wang, O. Mena, E. Di Valentino, and S. Gariazzo, arXiv:2405.03368 (2024), arXiv:2405.03368 [astro-ph.CO].
- [161] P. Brax, C. van de Bruck, E. Di Valentino, W. Giarè, and S. Trojanowski, *Mon. Not. Roy. Astron. Soc.* **527**, L122 (2023), arXiv:2303.16895 [astro-ph.CO].
- [162] P. Brax, C. van de Bruck, E. Di Valentino, W. Giarè, and S. Trojanowski, *Phys. Dark Univ.* **42**, 101321 (2023), arXiv:2305.01383 [astro-ph.CO].
- [163] D. Baumann, *Cosmology* (Cambridge University Press, 2022).
- [164] D. A. Dicus, E. W. Kolb, A. M. Gleeson, E. C. G. Sudarshan, V. L. Teplitz, and M. S. Turner, *Phys. Rev. D* **26**, 2694 (1982).
- [165] A. D. Dolgov and M. Fukugita, *Phys. Rev. D* **46**, 5378 (1992).
- [166] K. Akita and M. Yamaguchi, *JCAP* **08**, 012 (2020), arXiv:2005.07047 [hep-ph].
- [167] J. Froustey, C. Pitrou, and M. C. Volpe, *JCAP* **12**, 015 (2020), arXiv:2008.01074 [hep-ph].
- [168] J. J. Bennett, G. Buldgen, P. F. De Salas, M. Drewes, S. Gariazzo, S. Pastor, and Y. Y. Y. Wong, *JCAP* **04**, 073 (2021), arXiv:2012.02726 [hep-ph].
- [169] Z. Hou, R. Keisler, L. Knox, M. Millea, and C. Reichardt, *Physical Review D* **87** (2013), 10.1103/physrevd.87.083008.
- [170] J. Lesgourgues and S. Pastor, *Phys. Rept.* **429**, 307 (2006), arXiv:astro-ph/0603494.
- [171] S. Hannestad and T. Schwetz, *JCAP* **11**, 035 (2016), arXiv:1606.04691 [astro-ph.CO].
- [172] J. Lesgourgues and S. Pastor, *Adv. High Energy Phys.* **2012**, 608515 (2012), arXiv:1212.6154 [hep-ph].
- [173] J. Lesgourgues, G. Mangano, G. Miele, and S. Pastor, *Neutrino Cosmology* (Cambridge University Press, 2013).
- [174] S. Sarkar, *Rept. Prog. Phys.* **59**, 1493 (1996), arXiv:hep-ph/9602260.
- [175] N. Aghanim *et al.* (Planck), *Astron. Astrophys.* **641**, A5 (2020), arXiv:1907.12875 [astro-ph.CO].
- [176] N. Aghanim *et al.* (Planck), *Astron. Astrophys.* **641**, A8 (2020), arXiv:1807.06210 [astro-ph.CO].
- [177] J. L. Bernal, L. Verde, and A. G. Riess, *JCAP* **10**, 019 (2016), arXiv:1607.05617 [astro-ph.CO].
- [178] G. E. Addison, D. J. Watts, C. L. Bennett, M. Halpern, G. Hinshaw, and J. L. Weiland, *Astrophys. J.* **853**, 119 (2018), arXiv:1707.06547 [astro-ph.CO].
- [179] P. Lemos, E. Lee, G. Efstathiou, and S. Gratton, *Mon. Not. Roy. Astron. Soc.* **483**, 4803 (2019), arXiv:1806.06781 [astro-ph.CO].
- [180] K. Aylor, M. Joy, L. Knox, M. Millea, S. Raghunathan, and W. L. K. Wu, *Astrophys. J.* **874**, 4 (2019), arXiv:1811.00537 [astro-ph.CO].
- [181] N. Schöneberg, J. Lesgourgues, and D. C. Hooper, *JCAP* **10**, 029 (2019), arXiv:1907.11594 [astro-ph.CO].
- [182] L. Knox and M. Millea, *Phys. Rev. D* **101**, 043533 (2020), arXiv:1908.03663 [astro-ph.CO].
- [183] N. Arendse *et al.*, *Astron. Astrophys.* **639**, A57 (2020), arXiv:1909.07986 [astro-ph.CO].
- [184] G. Efstathiou, *Mon. Not. Roy. Astron. Soc.* **505**, 3866 (2021), arXiv:2103.08723 [astro-ph.CO].
- [185] R.-G. Cai, Z.-K. Guo, S.-J. Wang, W.-W. Yu, and Y. Zhou, *Phys. Rev. D* **105**, L021301 (2022), arXiv:2107.13286 [astro-ph.CO].
- [186] R. E. Keeley and A. Shafieloo, *Phys. Rev. Lett.* **131**, 111002 (2023), arXiv:2206.08440 [astro-ph.CO].
- [187] J.-Q. Jiang, D. Pedrotti, S. S. da Costa, and S. Vagnozzi, (2024), arXiv:2408.02365 [astro-ph.CO].
- [188] G. C. Carvalho, A. Bernui, M. Benetti, J. C. Carvalho, and J. S. Alcaniz, *Phys. Rev. D* **93**, 023530 (2016), arXiv:1507.08972 [astro-ph.CO].
- [189] E. de Carvalho, A. Bernui, G. C. Carvalho, C. P. Novaes, and H. S. Xavier, *JCAP* **04**, 064 (2018), arXiv:1709.00113 [astro-ph.CO].
- [190] G. C. Carvalho, A. Bernui, M. Benetti, J. C. Carvalho, E. de Carvalho, and J. S. Alcaniz, *Astropart. Phys.* **119**, 102432 (2020), arXiv:1709.00271 [astro-ph.CO].
- [191] D. Camarena and V. Marra, *Mon. Not. Roy. Astron. Soc.* **495**, 2630 (2020), arXiv:1910.14125 [astro-ph.CO].
- [192] R. C. Nunes, S. K. Yadav, J. F. Jesus, and A. Bernui, *Mon. Not. Roy. Astron. Soc.* **497**, 2133 (2020), arXiv:2002.09293 [astro-ph.CO].
- [193] R. C. Nunes and A. Bernui, *Eur. Phys. J. C* **80**, 1025 (2020), arXiv:2008.03259 [astro-ph.CO].
- [194] E. de Carvalho, A. Bernui, F. Avila, C. P. Novaes, and J. P. Nogueira-Cavalcante, *Astron. Astrophys.* **649**, A20 (2021), arXiv:2103.14121 [astro-ph.CO].
- [195] D. Staicova and D. Benisty, *Astron. Astrophys.* **668**, A135 (2022), arXiv:2107.14129 [astro-ph.CO].
- [196] R. Menote and V. Marra, *Mon. Not. Roy. Astron. Soc.* **513**, 1600 (2022), arXiv:2112.10000 [astro-ph.CO].
- [197] D. Benisty, J. Mifsud, J. Levi Said, and D. Staicova, *Phys. Dark Univ.* **39**, 101160 (2023), arXiv:2202.04677 [astro-ph.CO].
- [198] R. Shah, S. Saha, P. Mukherjee, U. Garain, and S. Pal, *Astrophys. J. Suppl.* **273**, 27 (2024), arXiv:2401.17029 [astro-ph.CO].
- [199] A. Favale, A. Gómez-Valent, and M. Migliaccio, *Phys. Lett. B* **858**, 139027 (2024), arXiv:2405.12142 [astro-ph.CO].
- [200] Ruchika, (2024), arXiv:2406.05453 [astro-ph.CO].
- [201] W. Giarè, J. Betts, C. van de Bruck, and E. Di Valentino, (2024), arXiv:2406.07493 [astro-ph.CO].
- [202] J. L. Bernal, T. L. Smith, K. K. Boddy, and M. Kamionkowski, *Phys. Rev. D* **102**, 123515 (2020), arXiv:2004.07263 [astro-ph.CO].
- [203] S. Sanz-Wuhl, H. Gil-Marín, A. J. Cuesta, and L. Verde, *JCAP* **05**, 116 (2024), arXiv:2402.03427 [astro-ph.CO].
- [204] J. Pan, D. Huterer, F. Andrade-Oliveira, and C. Avestruz, *JCAP* **06**, 051 (2024), arXiv:2312.05177 [astro-ph.CO].
- [205] M. Vargas-Magaña *et al.* (BOSS), *Mon. Not. Roy. Astron. Soc.* **477**, 1153 (2018), arXiv:1610.03506 [astro-ph.CO].
- [206] E. Sanchez, A. Carnero, J. Garcia-Bellido, E. Gaztanaga, F. de Simoni, M. Crocce, A. Cabre, P. Fosalba, and D. Alonso, *Mon. Not. Roy. Astron. Soc.* **411**, 277 (2011), arXiv:1006.3226 [astro-ph.CO].
- [207] D. Scolnic *et al.*, *Astrophys. J.* **938**, 113 (2022), arXiv:2112.03863 [astro-ph.CO].
- [208] Y. Toda, W. Giarè, E. Özülker, E. Di Valentino, and S. Vagnozzi, *Phys. Dark Univ.* **46**, 101676 (2024),

- arXiv:2407.01173 [astro-ph.CO].
- [209] J. Lesgourgues, (2011), arXiv:1104.2932 [astro-ph.IM].
- [210] B. Audren, J. Lesgourgues, K. Benabed, and S. Prunet, *JCAP* **02**, 01 (2012), arXiv:1210.7183 [astro-ph.CO].
- [211] T. Brinckmann and J. Lesgourgues, *Phys. Dark Univ.* **24**, 100260 (2019), arXiv:1804.07261 [astro-ph.CO].
- [212] A. Gelman and D. B. Rubin, *Statist. Sci.* **7**, 457 (1992).
- [213] A. Heavens, Y. Fantaye, E. Sellentin, H. Eggers, Z. Hosenie, S. Kroon, and A. Mootoivaloo, *Phys. Rev. Lett.* **119**, 101301 (2017), arXiv:1704.03467 [astro-ph.CO].
- [214] A. Heavens, Y. Fantaye, A. Mootoivaloo, H. Eggers, Z. Hosenie, S. Kroon, and E. Sellentin, (2017), arXiv:1704.03472 [stat.CO].
- [215] R. E. Kass and A. E. Raftery, *J. Am. Statist. Assoc.* **90**, 773 (1995).
- [216] R. Trotta, *Contemp. Phys.* **49**, 71 (2008), arXiv:0803.4089 [astro-ph].
- [217] A. G. Riess, L. Breuval, W. Yuan, S. Casertano, L. M. Macri, J. B. Bowers, D. Scolnic, T. Cantat-Gaudin, R. I. Anderson, and M. C. Reyes, *Astrophys. J.* **938**, 36 (2022), arXiv:2208.01045 [astro-ph.CO].
- [218] D. Camarena and V. Marra, *Mon. Not. Roy. Astron. Soc.* **504**, 5164 (2021), arXiv:2101.08641 [astro-ph.CO].
- [219] E. Aver, K. A. Olive, and E. D. Skillman, *JCAP* **07**, 011 (2015), arXiv:1503.08146 [astro-ph.CO].
- [220] B. D. Fields, K. A. Olive, T.-H. Yeh, and C. Young, *JCAP* **03**, 010 (2020), [Erratum: *JCAP* 11, E02 (2020)], arXiv:1912.01132 [astro-ph.CO].
- [221] V. Mossa *et al.*, *Nature* **587**, 210 (2020).
- [222] C. Pitrou, A. Coc, J.-P. Uzan, and E. Vangioni, *Mon. Not. Roy. Astron. Soc.* **502**, 2474 (2021), arXiv:2011.11320 [astro-ph.CO].
- [223] M.-M. Zhao, Y.-H. Li, J.-F. Zhang, and X. Zhang, *Mon. Not. Roy. Astron. Soc.* **469**, 1713 (2017), arXiv:1608.01219 [astro-ph.CO].
- [224] J.-Q. Jiang, W. Giarè, S. Gariazzo, M. G. Dainotti, E. Di Valentino, O. Mena, D. Pedrotti, S. S. da Costa, and S. Vagnozzi, (2024), arXiv:2407.18047 [astro-ph.CO].
- [225] W. Yang, E. Di Valentino, O. Mena, and S. Pan, *Phys. Rev. D* **102**, 023535 (2020), arXiv:2003.12552 [astro-ph.CO].
- [226] E. Di Valentino, S. Pan, W. Yang, and L. A. Anchordoqui, *Phys. Rev. D* **103**, 123527 (2021), arXiv:2102.05641 [astro-ph.CO].
- [227] E. Di Valentino, S. Gariazzo, C. Giunti, O. Mena, S. Pan, and W. Yang, *Phys. Rev. D* **105**, 103511 (2022), arXiv:2110.03990 [astro-ph.CO].
- [228] G. Steigman, *Adv. High Energy Phys.* **2012**, 268321 (2012), arXiv:1208.0032 [hep-ph].
- [229] I. J. Allali, M. P. Hertzberg, and F. Rompineve, *Phys. Rev. D* **104**, L081303 (2021), arXiv:2104.12798 [astro-ph.CO].
- [230] L. A. Anchordoqui, E. Di Valentino, S. Pan, and W. Yang, *JHEAp* **32**, 28 (2021), arXiv:2107.13932 [astro-ph.CO].
- [231] N. Khosravi and M. Farhang, *Phys. Rev. D* **105**, 063505 (2022), arXiv:2109.10725 [astro-ph.CO].
- [232] S. J. Clark, K. Vattis, J. Fan, and S. M. Koushiappas, *Phys. Rev. D* **107**, 083527 (2023), arXiv:2110.09562 [astro-ph.CO].
- [233] H. Wang and Y.-S. Piao, *Phys. Lett. B* **832**, 137244 (2022), arXiv:2201.07079 [astro-ph.CO].
- [234] L. A. Anchordoqui, V. Barger, D. Marfatia, and J. F. Soriano, *Phys. Rev. D* **105**, 103512 (2022), arXiv:2203.04818 [astro-ph.CO].
- [235] Y.-H. Yao and X.-H. Meng, *Commun. Theor. Phys.* **76**, 075401 (2024), arXiv:2312.04007 [astro-ph.CO].
- [236] S. S. da Costa, D. R. da Silva, A. S. de Jesus, N. Pinto-Neto, and F. S. Queiroz, *JCAP* **04**, 035 (2024), arXiv:2311.07420 [astro-ph.CO].
- [237] H. Wang and Y.-S. Piao, (2024), arXiv:2404.18579 [astro-ph.CO].
- [238] N. Craig, D. Green, J. Meyers, and S. Rajendran, *JHEP* **09**, 097 (2024), arXiv:2405.00836 [astro-ph.CO].
- [239] D. Green and J. Meyers, (2024), arXiv:2407.07878 [astro-ph.CO].
- [240] W. Elbers, C. S. Frenk, A. Jenkins, B. Li, and S. Pascoli, (2024), arXiv:2407.10965 [astro-ph.CO].
- [241] L. Herold, E. G. M. Ferreira, and L. Heinrich, (2024), arXiv:2408.07700 [astro-ph.CO].
- [242] S.-F. Ge and L. Tan, (2024), arXiv:2409.11115 [hep-ph].